Anchor Points: Benchmarking Models with Much Fewer Examples

Rajan Vivek, Kawin Ethayarajh, Diyi Yang, Douwe Kiela
Stanford University
{rvivek, kawin, diyiy, dkiela}@stanford.edu

Abstract

Modern language models often exhibit powerful but brittle behavior, leading to the development of larger and more diverse benchmarks to reliably assess their behavior. Here, we suggest that model performance can be benchmarked and elucidated with much smaller evaluation sets. We first show that in six popular language classification benchmarks, model confidence in the correct class on many pairs of points is strongly correlated across models. We build upon this phenomenon to propose *Anchor Point Selection*, a technique to select small subsets of datasets that capture model behavior across the entire dataset. Anchor points reliably rank models: across 87 diverse language model-prompt pairs, evaluating models using 1-30 anchor points outperforms uniform sampling and other baselines at accurately ranking models. Moreover, just a dozen anchor points can be used to estimate model per-class predictions on all other points in a dataset with low error, sufficient for gauging where the model is likely to fail. Lastly, we present *Anchor Point Maps* for visualizing these insights and facilitating comparisons of the performance of different models on various regions within the dataset distribution.

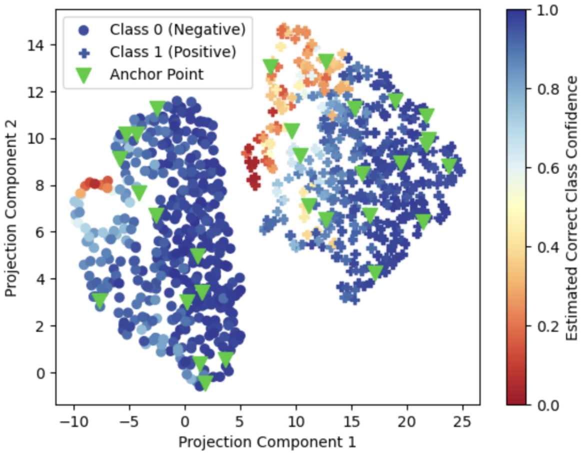

Figure 1: SST-2 Validation Set Anchor Point Map. The locations of all 872 points are learned using the predictions of 60 randomly-selected source models on SST-2. We then evaluate a held-out model, Falcon-7B, on 30 anchor points (green triangles). The model's predictions on only these 30 points are used to estimate the Falcon-7B predictions on the remaining 842 points with a mean absolute error of 0.09, achieving 92% agreement with the model's true predictions. The anchor points identify regions where the model is weak (red regions). We show the same Anchor Point Map colored by the true Falcon-7B predictions in Figure 9, demonstrating that the model is indeed weak in these areas.

1 Introduction

Language models have unlocked incredible generalization through scaling up parameters and pretraining data. Yet these same systems prove to be brittle, spurring the development of larger, more diverse, and more shrewd benchmarks to reliably assess their behavior (Rajpurkar et al., 2016; Hendrycks et al., 2021; Kiela et al., 2021; Wu et al., 2023). Modern benchmarks typically have on the order of 10^5 validation examples, with $10^3 - 10^4$ per task. Such numbers ensure that validation performance strongly correlates with test performance and that all in-domain regions are captured. But these sizes are often unwieldy for rapid experimentation and do not easily afford interpretability. To compare model configurations, design the most robust prompt, or analyze failure cases, researchers and practitioners must forward-pass (and potentially manually inspect) the development set many times. How small can benchmark development sets be while still capturing model behavior over the full breadth of the benchmark? Surprisingly, very small—just several to a few dozen examples might suffice.

In this work, we investigate the problem of benchmarking model performance and revealing model weaknesses on large datasets with as few evaluation examples as possible, an objective we call *micro-benchmarking*. We propose *Anchor*

Proceedings of the 18th Conference of the European Chapter of the Association for Computational Linguistics
Volume 1: Long Papers, pages 1576–1601
March 17-22, 2024 ©2024 Association for Computational Linguistics

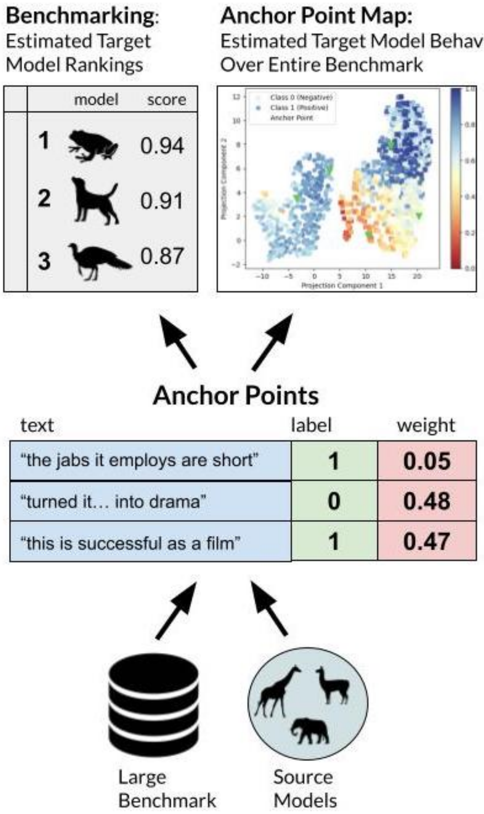

text	label	weight
"the jabs it employs are short"	1	0.05
"turned it… into drama"	0	0.48
"this is successful as a film"	1	0.47

Figure 2: Anchor Points are Micro-Benchmarks, tiny representative subsets of large benchmarks. Correlative structure in the predictions of source models on the large benchmark can be used to extract these points. Each anchor point has a weight corresponding to the fraction of the benchmark it represents. Evaluating models on the anchor points produces a score that rank correlates with performance on the entire benchmark. Anchor Point Maps visualize a given model's likely instance-level performance on all points in the benchmark using only its performance on the anchor points.

Point Selection, a technique that finds small evaluation sets that are maximally representative of model behavior over the entirety of a large dataset. We find that anchor points are effective development sets: across 87 diverse language models and prompts, using 1-30 anchor points shows superior performance at ranking model performance over random and embedding-based selection baselines. Moreover, evaluating just a dozen anchor points can be used to predict the model's instance-level predictions on all other points in the dataset with high agreement on average, sufficient to estimate where models are likely to fail.

Our approach builds upon a simple insight: for many pairs of points from a given dataset, the predicted probability of the correct class strongly correlates across models. Thus, evaluating every model on the entirety of a dataset is redundant. The predictions of existing *source* models on a given dataset are telling about predictions of a new *target* model, even across considerable performance gaps. This mirrors phenomena like *Accuracy on the Line* (Miller et al., 2021) and *Agreement on the Line* (Baek et al., 2022), but at a much more granular scale. Anchor Points can be selected by identifying dataset medoids in a space where distance is a positive, monotonically decreasing function of cross-model correlations between points. We further propose to visualize this space using multidimensional scaling and U-MAP (McInnes et al., 2018), which we call *Anchor Point Maps*. Anchor Point Maps show what region each anchor point captures and highlight that different models and prompts may struggle on different dataset regions, allowing fine-grained comparisons.

Emphatically, we do not aim to replace large benchmarks, but rather provide cheaper signal about model performance on these benchmarks to help accelerate the development of models and prompts. We also strive to be blunt about the limitations of our technique. Anchor point generalization relies on the predictive correlations of source models being consistent with that of target models. This is not always the case, leading to poor generalization to specific target models depending on the choice of source models. We share simple rules of thumb to promote this source-target consistency, but lack rigorous theory to guide source model selection. We lay foundations for further research into model predictive correlations and efficient, interpretable model evaluation.

2 Related Work

Sample-Efficient Model Evaluation We deviate from prior sample-efficient model evaluation literature along key axes. Many works (Kossen et al., 2021a,b; Deng and Zheng, 2021; Corneanu et al., 2020) minimize evaluation *annotation* costs by actively selecting points to annotate for evaluating a given model. In the era of large benchmarks and large models, labeled evaluation examples are widely-available but evaluating all of them is cumbersome. Our technique instead minimizes the number of *forward-passed examples* necessary for reliable model evaluation. Furthermore, our selection strategy is agnostic to the target model(s) being evaluated. The resulting evaluation set is transferable to other language models.

Other works (Rodriguez et al., 2021; Ethayarajh et al., 2022; Bowman and Dahl, 2020) point out that it is often a minority of points that differentiate the performance of various models. Rodriguez et al. (2021) show that evaluating models on points identified as the most *discriminative* can effectively rank model performance. However, optimizing for discriminability does not result in representative subsets: very easy or very hard points will tend to be excluded, leading to a different distribution. Instead, we optimize for *representativeness* which we show naturally leads to discriminability.

Instance-Level Model Performance Despite being noisy (Zhong et al., 2021), instance-level model predictions are a rich source of information about model behavior. Swayamdipta et al. (2020) present Data Maps, a powerful technique that leverages instance-level predictions to reveal underlying structure in the interplay of models and data points. Various training example regions play distinct roles in guiding a classifier to its solution. Unlike our technique, Data Maps are not used for comparing model performance or isolating distinct regions of the dataset distribution where models are weak.

Ethayarajh et al. (2022) further show that instance-level predictions can be used to quantify how much information a given model can extract from a dataset, providing a formal metric of dataset difficulty that exposes model behavior at the dataset and data point level.

Predictive Correlations across Models Miller et al. (2021) present the *Accuracy on the Line* phenomenon: out-of-distribution (OOD) performance is strongly positively correlated with in-distribution (ID) performance for a wide range of models and distribution shifts. This unexplained by classical theory which provides only weak bounds relating the two metrics (Ben-David et al., 2018). Baek et al. (2022) further show that the *agreement* of two classifiers on ID data strongly linearly correlates with their agreement on OOD data whenever *Accuracy on the Line* holds. Both phenomena can be used to cheaply estimate model OOD performance. Our findings presented in this work mirror these phenomena at a much more granular scale, i.e., data instances rather than data sets.

Coresets Anchor Points can be interpreted as a coreset, broadly defined as a small "summary" of a large set of data (Feldman, 2020; Guo et al., 2022). Selecting dataset coresets for efficient model training is widely-explored in prior work, performed through various techniques including clustering (Kaufman and Rousseeuw, 2009; Reza Zanjirani Farahani, 2009), gradient-matching (Mirzasoleiman et al., 2020; Killamsetty et al., 2021a), bi-level optimization (Borsos et al., 2020; Killamsetty et al., 2021b), and submodularity-based methods (Kai Wei, 2015). We use a clustering-based approach, but focus on summarizing data for model *evaluation* rather than training.

3 Problem Set-Up

Let $\mathcal{D} = \{(x_i, y_i)\}_{i=1}^{K}$ be a language classification benchmark. $\mathcal{D}$ is partitioned into a training split $\mathcal{D}_{train}$ and one or more evaluation splits $\mathcal{D}_{eval}$, each drawn i.i.d from $\mathcal{D}$. We are given M models to evaluate, denoted as the target set $\mathcal{T} = \{\phi_m\}_{m=1}^{M}$. Each unique ϕ_m corresponds to a model fine-tuned on $\mathcal{D}_{train}$ or paired with a specific prompt template that directs the model at solving $\mathcal{D}$. The dataset has an evaluation metric (accuracy, F1-score, etc.) to measure the aggregate performance P_m of each ϕ_m on an evaluation split $\mathcal{D}_{eval}$.

We additionally have access to the instance-level predictions of a source set of N model and prompt template pairs $\mathcal{S} = \{\phi_n\}_{n=1}^{N}$ over the entirety of $\mathcal{D}_{eval}$. $\mathcal{S}$ and $\mathcal{T}$ are disjoint. The predictions occupy an $N \times |\mathcal{D}_{eval}| \times Y$ tensor $P_{\mathcal{S}}$, where Y is the cardinality of the classification task. In practice, source models could be open-source models that can be run locally for free while target models might be closed-source and/or more expensive.

Towards Micro-Benchmarking We aim to extract a development set from a large benchmark that captures the benchmark's broad coverage and reliable ranking power while being as small as possible, improving performance interpretability and evaluation efficiency. We refer to this objective as **micro-benchmarking**. The technique must 1) acquire a small representative subset of evaluation points from the large benchmark ($X_{acq} \subseteq \mathcal{D}_{eval}, |X_{acq}| \ll |\mathcal{D}_{eval}|$), 2) leverage the predictions of target models $\{\phi_m\}_{m=1}^{M}$ on the subset to produce scores $S_{1...M}$ that correlate as much as possible with model performances $P_{1...M}$ on the entire dataset $\mathcal{D}_{eval}$, and 3) estimate instance-level performance on untested points from $\mathcal{D}_{eval}$.

4 Micro-Benchmarking Approach

We measure how well an example (x_1, y_1) represents another example using the Pearson correlation of correct class confidence in the two examples measured across the predictions of the source models in $\mathcal{S} = \{\phi_n\}_{n=1}^{N}$. If our data is not annotated, we can instead compute $\mathcal{Y}$ Pearson correlations (one across each class) per example pair and average them. However, model confidences are bounded by [0, 1] and thus can only follow a linear trend for a bounded range. Akin to Miller et al. (2021), we take the logit transform of the confidences to scale the axes from [0,1] to $[-\inf, +\inf]$ prior to computing correlations. We denote this composite function as $CORR_{\mathcal{S}}$. The task of selecting a X_{acq} that is maximally representative of D_{eval} for all models in $\mathcal{S}$ reduces to solving a K-Medoids problem that maximizes the correlation between the selected and the remaining points:

$$\min_{X_{acq}} \sum_{i=1}^{B} \sum_{x_{eval}^{j} \in Q_i} 1 - CORR_{\mathcal{S}}(x_{acq}^{i}, x_{eval}^{j}) \quad (1)$$

where B is the number of anchor points and Q_i is the set containing all x_{eval} that are more strongly correlated with x_{acq}^{i} than any other x_{acq}^{j}. This objective makes the assumption that the estimate for $\phi_m(x_{eval})$ leverages only the most strongly correlated $\phi_m(x_{acq}^{i})$. We efficiently solve this objective using the Partitioning Around Medoids (PAM) algorithm (Kaufman and Rousseeuw, 2009).

4.1 Anchor Point Techniques

We present two techniques for leveraging anchor points to benchmark model performance with minimal evaluation examples.

Technique 1: Anchor Point Predictor We propose the Anchor Points Predictor, an ensemble of univariate linear regression models that use model predictions on each anchor point to estimate predictions on all other points in X_{eval}. Specifically, anchor point $\phi(x_{acq}^{i})$ is used to estimate all $\phi(x_{eval}) \in Q_i$. These instance-level prediction estimates can then be used to detect regions of model weaknesses (see Section 4.1) and compute an estimate of any performance metric for the target model. This technique requires that the trend lines fitted to source model predictions explains the variance in target model predictions well. We explore when this is the case in Appendix A. Algorithms 1 and 2 show pseudocode for fitting and making predictions with the Anchor Point Predictor Model.

Technique 2: Anchor Point Weighted Score Rather than attempting to estimate exact model performance at the instance-level, we can aim to produce a score for each target model that highly correlates with the model's performance on $\mathcal{D}_{eval}$. Using the predictions of the source model set $\mathcal{S}$, we select $N \in 1...B$ anchor points according to Equation 1. Each of these points $x_{acq,i}$ strongly correlates with a subset of the untested points in $\mathcal{D}_{eval}$, namely all $x_{eval}^{j} \in Q_i$. We propose the Anchor Point Weighted (APW) score, a weighted average of the model's correct class probability predictions on the anchor points with weights proportional to cluster size.

$$APW(\phi_i) = \frac{1}{|\mathcal{D}_{eval}|} \sum_{i=1}^{B} |Q_i| * \phi_i(x_{acq}^{i})[y_i] \quad (2)$$

Anchor Point Maps To highlight the insights provided by anchor points, namely model strengths and weaknesses in distinct regions of a dataset, we propose to visualize the cross-model correlative space from which anchor points are drawn. We compute pairwise correlations between all points using $CORR_{\mathcal{S}}$, creating a $|\mathcal{D}_{eval}| \times |\mathcal{D}_{eval}|$ correlation matrix C. We then represent the distance matrix Z as a positive, monotonically decreasing function of correlation: $Z = 1 - C$. Finally, we cast the points to a high-dimensional continuous space using Multi-Dimensional Scaling on Z and project the space to two components with U-MAP (McInnes et al., 2018). This technique visualizes the dataset in a space where a model's performance on each point generalizes to the local neighborhood of that point.

5 Predictive Correlations

To motivate our approach, we first show that language models make predictions with consistent structure. For many pairs of points from a given dataset, the predicted probability of the correct class strongly correlates across models.

Experimental Set-Up We obtain a diverse set of language models from HuggingFace and the OpenAI API: 27 BERT-family models, 11 non-instruction-tuned GPT-family models, 5 instruction-tuned GPT-family models, and 5 GPT-3/3.5 variants (all listed in Tables 9 - 10). We denote these model sets as the BERT-family, GPT-family, InstructGPT-family, and OpenAI-family

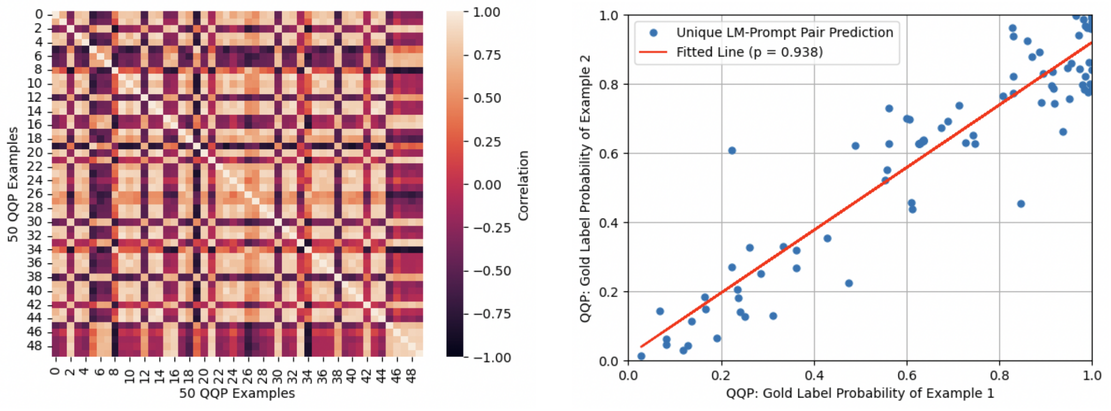

(a) Pairwise Correlation Matrix of ALL-Family Correct Class Confidences on 50 QQP Examples. Rich structure indicates the relatedness of various examples. Many are strongly correlated.

(b) Correct Class Confidences of 87 Language Model Predictions from all model families on Two Selected QQP examples. A model correctly classifying one example is predictive of the model correctly classifying the other. This phenomenon is very common.

Figure 3: Predictive Correlations at the Instance-Level Across Language Models

respectively. For six datasets from the GLUE benchmark (Wang et al., 2019), we finetune each BERT-family model on the training split $\mathcal{D}_{train}$ and obtain its predicted probability of the correct class on each instance in the validation split $\mathcal{D}_{eval}$. For the other model families we zero-shot prompt for the same datasets using three multiple-choice prompts per dataset (Appendix D). We obtain the predicted probability of each class by performing softmax over the log probabilities of candidate answer sequences. Thus, we obtain a prediction matrix P for each model family and dataset with size $N_{subjects} \times |\mathcal{D}_{eval}|$ matrix where $N_{subjects} = 27$ for P_{BERT}, 30 for P_{GPT}, 15 for P_{IGPT}, 15 for P_{OAI}, and 87 for their union P_{ALL}.

Model predictions on pairs of examples are linearly correlated across models. The prediction matrices are approximately low-rank for all tasks (Table 1). This can be attributed to a simple phenomenon: let $\phi_n(x_1)[y]$ denote the probability mass (equivalently, model confidence) outputted by ϕ_n on $x_1 \sim \mathcal{D}_{eval}$ for a given class y. We see that $\phi_n(x_1)[y]$ often linearly correlates with the model's prediction on a different instance $\phi_n(x_2)[y]$ across models, i.e. $\phi_n(x_2)[y] \approx w\phi_n(x_1)[y] + b$, where w and b can be found by fitting a trend line through the correct class confidences of all source models.

Figure 3 visualizes this phenomenon. We first observe that the correlation matrices of model predictions on the same evaluation set show rich structure. Figure 3(b) shows a QQP example pair that is strongly positively correlated across models from all families. This suggests that evaluating a model on both examples is redundant. This phenomenon is wide-spread: it holds for many pairs of examples across the six GLUE tasks and 87 widely-used language models and prompts.

Predictive Correlations Tend to Generalize Across Diverse Models Figure 6 in Appendix A shows how well the strong trends from each family transfer to other families. Errors are lowest in the bottom row, suggesting that using source models that span all model families result in the most generalizable trend lines. We also observe that the predictive correlations of the BERT-family do not generalize well to other model families, which we explore further in Figure 8(b). However, most errors in the table are generally low, suggesting that predictive correlations tend to generalize across diverse models.

6 Sample-Efficient Model Evaluation

We now evaluate the anchor point techniques and compare against baselines for 1) selecting representative evaluation subsets to rank models[1] and 2) estimating model instance-level performance on held-out points in $\mathcal{D}_{eval}$.

Subset Selection Baselines and Metrics For baselines, we use uniform random sampling as well as K-Medoids sampling over the embedding

[1] We also evaluate anchor point techniques for ranking MMLU performance in Appendix B

Task	BERT	GPT	IGPT	OAI	ALL
MNLI	$2_{0.1}$	$1_{0.07}$	$3_{0.07}$	$4_{0.1}$	$3_{0.09}$
SST-2	$1_{0.08}$	$2_{0.05}$	$2_{0.09}$	$3_{0.1}$	$2_{0.09}$
QQP	$2_{0.06}$	$2_{0.06}$	$2_{0.1}$	$4_{0.09}$	$3_{0.09}$
RTE	$2_{0.07}$	$2_{0.06}$	$2_{0.08}$	$3_{0.1}$	$2_{0.08}$
MRPC	$2_{0.08}$	$4_{0.1}$	$3_{0.09}$	$7_{0.1}$	$7_{0.1}$
QNLI	$1_{0.08}$	$2_{0.08}$	$3_{0.09}$	$7_{0.09}$	$3_{0.09}$

Table 1: Approximate matrix rank of the correct class probability predictions of four model families on six GLUE task validation sets. We compute low-rank matrix approximations for 27 BERT-family predictions, 30 GPT-family predictions, 15 Instruction-tuned GPT-family predictions (IGPT), 15 OpenAI-family predictions (OAI), and all 87 model predictions (ALL) together. The approximations achieve very low mean absolute error (indicated by the subscripts), despite their ranks being considerably smaller than the number of models in each family.

spaces of a generic sentence encoder– Sentence-BERT (Reimers and Gurevych., 2019) – and an encoder fine-tuned on the dataset– the *CLS* token of bert-base-uncased (Devlin et al., 2018). For these techniques, we use model performance on the selected points as the estimate of aggregate model performance on the entire dataset. We further consider variants of these baselines that consider model confidence. We propose mean model confidence in the correct class on randomly selected points as one baseline. We also propose to produce a score estimate for each model by computing a weighted average of the correct class probabilities assigned to each selected point. The weights are proportional to the size of each selected point's cluster and sum to 1, akin to Anchor Points Weighted.

To assess the ranking performance of each technique, we compute the Kendall rank correlation coefficient (Kendall's τ) for a range of anchor point set sizes and report the resulting **Area Under the Correlation Curve** (AUCC) from 1 to a maximum budget B. We then normalize AUCC by dividing by the best possible area. In the experiments we use $B = 30$, the small data regime for which it is reasonable for practitioners to manually inspect predictions.

Prediction Estimation Baselines and Metrics We consider two naive baselines: 1) using the instance-level predictions of a randomly selected source model on $\mathcal{D}_{eval}$ as the estimate of each target model's prediction and 2) using the mean prediction of all source models on each point in $\mathcal{D}_{eval}$ as the estimate. We also propose Nearest Source Neighbor, a strategy where each target model's predictions on k randomly selected points are compared to the predictions of all source models on the same points. We select the source model with the most similar predictions on these k points, as measured with $L1$-distance. The predictions of this source model on all other points in $\mathcal{D}_{eval}$ are then used as the estimate of the target model's predictions.

To measure the performance of each technique, we use *agreement*– the percentage of points for which the estimation technique assigns the highest probability to the same class as the target model.

Anchor Points Show Competitive Performance at Ranking Models with Small Evaluation Sets Table 2 shows the Kendal's τ AUCC of the methods for ranking 77 models belonging to all model families. These curves are shown in Figures 15 and 16. Table 7 shows performance within each model family. Overall, we observe that Anchor Points Weighted outperforms random selection in 29 of 30 settings and Anchor Points Predictor outperforms random selection in 27 of 30 settings. Anchor Points Weighted proves to be the strongest among all techniques, followed by Anchor Points Predictor. Very small anchor point sets achieve surprisingly strong correlation, serving as reliable evaluation sets that can easily be inspected by eye (e.g. Figure 11). Moreover, we still observe these gains when source models are freely-available while all target models are closed-source (Table 4).

Anchor Point Weighted Correlations Are Reliable, Unlike Strong Contenders We observe that Anchor Point Weighted (APW) performance tends to be more reliable across evaluation set sizes and test settings than APP as well as the baselines. We suspect APW is more reliable than APP because it makes a weaker assumption that source model predictions simply follow similar correlations as target model predictions rather than closely matching the exact regression line fitted to the source model predictions. This is corroborated by results in Appendix B with the MMLU dataset, where APW still demonstrates superior performance over baselines despite a small number of source models, but APP performance worsens.

We observe inconsistent and sometimes erratic behavior in the embedding-based baselines. Despite Fine-tuned and Fine-tuned Weighted base-

	Random	Random Mean	Pretrained	Pretrained Weighted	Fine-Tuned	Fine-Tuned Weighted	AP Weighted	AP Predictor
Datasets	Exact	Corr	Exact	Corr	Exact	Corr	Corr	Exact
SST-2	0.685	0.705	0.734	0.725	0.730	**0.787**	0.757	0.727
QQP	0.669	0.678	0.189	0.233	0.766	**0.770**	0.756	0.701
RTE	0.366	0.308	0.143	-0.052	0.354	0.275	**0.483**	0.462
QNLI	0.321	0.331	0.192	0.294	0.127	0.144	**0.439**	0.303
MRPC	0.687	0.679	0.528	0.604	0.641	0.681	**0.726**	0.716
MNLI	0.438	0.433	0.177	0.166	0.523	0.453	**0.544**	0.517
Average	0.528	0.522	0.327	0.328	0.523	0.518	**0.612**	0.571

Table 2: Area Under the (Kendall's τ) Correlation Curve from 1 to 30 points for ranking 77 language models at 6 General Language Understanding tasks (GLUE). We randomly select 10 models to be source models for the AP methods and rank the remaining 77 models, averaging over 100 randomized runs. AP Weighted and AP Predictor show significant gains, which are most dramatic at smaller evaluation sets (Figures 15 and 16). "Exact" indicates the method generates a score that is intended to approximate the true aggregate performance directly, while "Corr" indicates the method generates a score intended only to rank correlate with true performance. The best score is **bolded** and second best score is underlined. Table 7 shows these results broken down by model family.

lines collectively achieving the best performance in 10 settings, these baselines prove to be inconsistent: Fine-tuned and Fine-tuned Weighted perform worse than random in 12 and 10 settings, respectively. We suspect this is because language model embedding spaces are not always smooth and are likely to be inconsistent across models.

Anchor Points Efficiently Estimate Model Predictions The Anchor Point Predictor can estimate model performance at the instance-level over the entire dataset. Table 3 shows the average agreement between Anchor Point estimated instance-level model predictions and true model predictions using various numbers of anchor points and randomly selected source models. The estimates of a small number of anchor points achieve high average agreement with true model predictions. However, the source model correlations do not generalize well to all target models, resulting in lower agreement on these outlier models and thus large standard deviations in Table 3. As a general rule of thumb, selecting a source model set that is diverse (e.g. comes from multiple families, see Figure 6) results in the best generalization. Strategies for intelligently selecting source models are a promising direction to resolve poor anchor point generalization, which we discuss further in Appendix A.

Nearest Source Neighbor is a Strong Baseline Nearest Source Neighbor achieves competitive performance at estimating model instance-level predictions. The agreement achieved by this technique is upper bounded by the agreement of each target model and its true nearest source model neighbor (indicated by the $B = |\mathcal{D}_{eval}|$ column in Table 3). Surprisingly, comparing just $B = 10$ random points closely approaches this bound, suggesting that the similarity of the predictions of different models can be approximated cheaply. Note that using $B = 100$ anchor points surpasses the upper bound of this baseline on 3 of the 6 datasets.

7 Sample-Efficient Model Analysis

We now highlight how anchor point maps provide fine-grained analysis of model generalization both within and across datasets. This is achieved in a sample-efficient manner using the Anchor Point Predictor.

Anchor Point Maps Visualize Where Models Generalize Anchor Point Maps reveal the extent to which models learn distinct regions of dataset distributions. Model performance on each sample correlates with performance in the sample's neighborhood, allowing the Anchor Point Predictor to estimate where models will fail without evaluating the entire dataset. Figure 1 shows the SST-2 validation set mapped by the predictions of 60 source models and then colored by estimated Falcon-7B predictions using thirty anchor points. These estimated predictions are quite faithful to the model's true predictions (achieving 0.09 MAE and 92% agreement), revealing regions where the model is weak. This localization of model behavior starkly contrasts with typical language embedding spaces, where model performance tends to be non-localized (Figure 12). However, like embedding spaces, related examples naturally cluster together.

		Random Source	Mean Source	Nearest Source Neighbor		Anchor Points	
Dataset	$\lvert\mathcal{D}_{eval}\rvert$	$B = 0$	$B = 0$	$B = 10$	$B = \lvert\mathcal{D}_{eval}\rvert$	$B = 10$	$B = 100$
SST-2	872	$0.63_{0.23}$	$0.74_{0.17}$	$0.83_{0.16}$	$\mathbf{0.84_{0.15}}$	$0.83_{0.12}$	$\mathbf{0.84_{0.11}}$
QQP	6000	$0.54_{0.28}$	$0.59_{0.22}$	$0.84_{0.15}$	$\mathbf{0.85_{0.14}}$	$0.81_{0.13}$	$0.83_{0.14}$
RTE	277	$0.53_{0.32}$	$0.58_{0.31}$	$0.80_{0.21}$	$0.81_{0.20}$	$0.83_{0.17}$	$\mathbf{0.85_{0.16}}$
QNLI	5463	$0.60_{0.26}$	$0.65_{0.23}$	$0.78_{0.19}$	$\mathbf{0.79_{0.19}}$	$0.76_{0.17}$	$0.75_{0.15}$
MRPC	408	$0.53_{0.26}$	$0.56_{0.20}$	$0.80_{0.15}$	$0.82_{0.14}$	$0.79_{0.14}$	$\mathbf{0.84_{0.11}}$
MNLI	6000	$0.40_{0.30}$	$0.46_{0.28}$	$0.71_{0.26}$	$0.72_{0.25}$	$\mathbf{0.79_{0.20}}$	$0.76_{0.20}$
Average	–	0.54	0.60	0.79	**0.81**	0.80	**0.81**

Table 3: Agreement of true target model predictions and estimated target model predictions for anchor points and baselines, where B indicates the number of points the target models are evaluated on. We randomly select 10 models to be source models and estimate the predictions of the remaining 77 models, averaging over 100 randomized runs. Anchor Points and Nearest Source Neighbor surpass the naive baselines by a large margin. Standard deviations (subscripts) remain large, indicating the presence of outlier models. The $B = \lvert\mathcal{D}_{eval}\rvert$ column is shown only for reference to highlight that Anchor Points can surpass the upper bound of Nearest Source Neighbor performance. Note that standard errors can be computed by dividing the standard deviations by 10. The best score is **bolded**.

Anchor Points Predict Diverse Model Behavior Figure 5 in the Appendix shows four Anchor Point Maps of 1000 QQP points, comparing the true and estimated predictions of deberta-v3-base and text-davinci-003 using 30 anchor points. The two models are weak in distinct regions of the dataset. Despite deberta-v3-base achieving stronger performance overall, it fails in a region of the negative class cluster where text-davinci-003 is mostly correct. This is perhaps related to "no-free lunch" theorems in statistical learning theory: different models have biases that will lend them to perform the best on different inputs (Ben-David and Shalev-Shwartz, 2014), which is obscured by single-number evaluation metrics. The fact that the same set of anchor points can generalize to models with diverse behaviors highlights that the same underlying predictive correlations can engender these different behaviors. We explore anchor point generalization further in Appendix A.

Anchor Point Maps Reveal Patterns in Model Knowledge To explore the characteristics of anchor points beyond basic language understanding tasks, we generate an anchor point map (Figure 4(a)) using the predictions of 14 LLMs on 6 MMLU datasets (Hendrycks et al., 2021). Each dataset contains multiple choice questions from a distinct domain, requiring substantial real-world knowledge to answer. We observe overlap of all domains in the anchor point map, but there is a remarkable amount of structure: models tend to have correlated performance on groups of questions from the same domain as well as related domains. This is quantified is Figure 4(b), which shows the distribution of domains of each question type's 10 nearest neighbors. On average, around 60% of the nearest neighbors of a high school physics question are also from the high school physics domain. In contrast, a nearest neighbor of a college chemistry question is equally likely to be about college chemistry or clinical knowledge. This suggests that models with strong knowledge of college chemistry are likely to have strong knowledge of clinical knowledge as well. This is perhaps due to frequent co-occurrence of these subjects in pre-training data.

Anchor Points Capture Model Performance, Not Language Semantics Notably, Figure 4(b) reveals that high school physics and college physics questions are often not nearest neighbors, despite these datasets having the largest vocabulary overlap (21%) of any pair within the 6 MMLU datasets (Figure 14). This highlights that the semantic similarity of two questions is often a poor proxy for similar model performance on the questions, explaining why embedding-based approaches to sample-efficient model evaluation tend to fail. Anchor Point Selection is more akin to test-distribution aware active learning, where points are selected based on the information they provide about future model predictions (MacKay, 1992; Kirsch et al., 2021).

8 Limitations

Anchor Points Show Diminishing Returns We discuss in Appendix A that APW correlation begins to plateau as the evaluation set size grows to 100 points due to an inherent upper bound. We also discuss that for large evaluation sets, anchor points

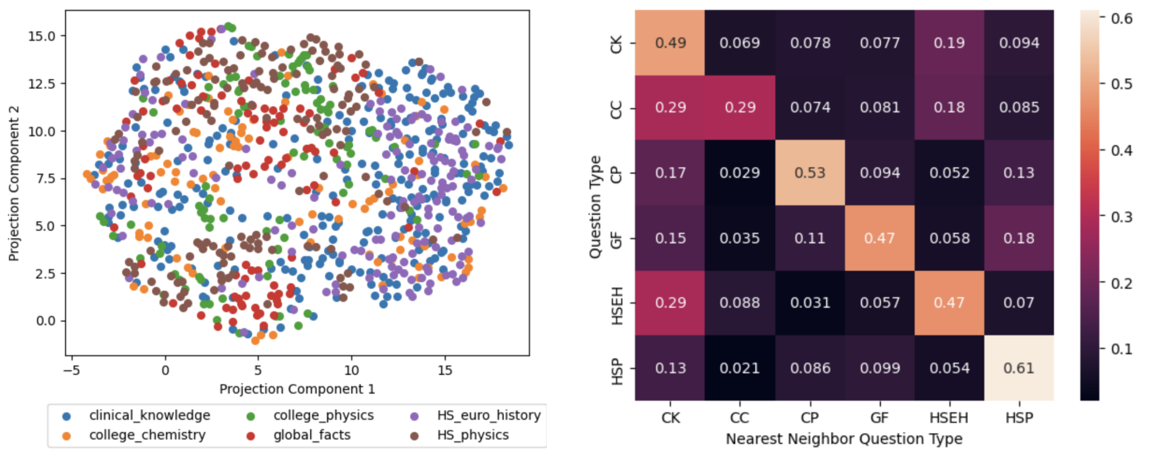

(a) Anchor Point Map of 6 Combined MMLU datasets. The map is computed using the predictions of 13 source models. We color each point according to the dataset to which it belongs. We observe that all datasets overlap, but points tend to cluster with other points from the same dataset or a related dataset.

(b) For each question type (i.e dataset), we show the distribution of question types of its 10 nearest neighbors (on average). For example, the top row shows that 49% of the nearest neighbors of clinical knowledge (CK) questions tend to also be clinical knowledge, while 19% tend to be high school European history (HSEH). Labels: CK = clinical knowledge, CC = college chemistry, CP = college physics, GF = global facts, HSES = high school European history, HSP = high school physics.

Figure 4: Analysing Patterns in Model Knowledge using MMLU Anchor Point Map.

can underperform random selection. More work is needed to develop methods that are robust to evaluation set size.

Anchor Points Do Not Always Generalize In order for anchor points and anchor point maps to generalize, the predictive trends of source models must be consistent with that of target models. While Table 7 shows that anchor points often transfer both within and across model families, the correlations of randomly selected source models do not necessarily generalize to all target models (e.g. Figure 13). We currently lack rigorous theory to guide source model selection for evaluation of a given set of target models.

Anchor Points Can be Further Optimized In its current form, Anchor Point Maps require computing correlations between all pairs of points in the dataset. This is computationally expensive for huge datasets. Multi-dimensional scaling with missing values or correlation matrix completion could dramatically decrease these costs.

9 Conclusion and Future Work

We present Anchor Point Selection, a technique that finds maximally-representative subsets from large datasets which can be used to efficiently rank models and estimate model behavior over the entire dataset. We also present Anchor Point Maps, a tool to visualize how well models generalize across various subsets of datasets.

Important future work includes developing better theory underlying when models share predictive correlations and designing intelligent source model selection strategies to ensure anchor point generalization to desired sets of target models.

The fact that diverse language models make highly correlated predictions on many pairs of examples suggests that modern benchmarks contain many redundant examples. An interesting future direction would be to use predictive correlations to guide benchmark development by selecting fewer redundant examples, which would ideally lead to more diverse and difficult benchmarks.

The potential to extend Anchor Point Maps and Anchor Point Selection to tasks beyond language classification is exciting. Perhaps other continuous performance metrics are strongly correlated between examples, such as BLEU scores or the rewards given by a reward model. Exploiting such phenomena could allow a dramatic reduction in the number of examples that modern language models must be evaluated on, leading to reduced costs for model development.

Ethics Statement

We aim to encourage the research community to consider how modern NLP models can be evaluated more efficiently. While this endeavor could ideally reduce the compute required to develop models, minimizing evaluation set size poses the risk of excluding minority subsets of the data distribution. This could harm model generalization and lead to reduced performance in rarer use cases, e.g. on low-resource languages. As an empirical example, observing where Figures 9(a) and 9(b) differ reveals a small subset of points in sparser regions that are poorly captured by the anchor points. We find that examples in this region remain poorly captured across random seeds and anchor point set sizes, highlighting a systematic lack of generalization to this minority subset.

To mitigate the risks of our work, we 1) emphasize that our ultimate goal is not to replace large benchmarks but rather provide cheaper signal about model benchmark performance and 2) remain candid about the limitations of our approach to lay the foundation for future work in efficient, robust model evaluation strategies.

References

Samira Abnar, Mostafa Dehghani, Behnam Neyshabur, and Hanie Sedghi. 2021. Exploring the limits of large scale pre-training. arXiv.

Stephen H. Bach, Victor Sanh, Zheng-Xin Yong, Albert Webson, Colin Raffel, Nihal V. Nayak, Abheesht Sharma, Taewoon Kim, M Saiful Bari, Thibault Fevry, Zaid Alyafeai, Manan Dey, Andrea Santilli, Zhiqing Sun, Srulik Ben-David, Canwen Xu, Gunjan Chhablani, Han Wang, Jason Alan Fries, Maged S. Al-shaibani, Shanya Sharma, Urmish Thakker, Khalid Almubarak, Xiangru Tang, Dragomir Radev, Mike Tian-Jian Jiang, and Alexander M. Rush. 2022. Promptsource: An integrated development environment and repository for natural language prompts. Association for Computational Linguistics.

Christina Baek, Yiding Jiang, Aditi Raghunathan, and Zico Kolter. 2022. Agreement-on-the-line: Predicting the performance of neural networks under distribution shift.

Elisa Bassignana, Max Müller-Eberstein, Mike Zhang, and Barbara Plank. 2022. Evidence > intuition: Transferability estimation for encoder selection.

Shai Ben-David, John Blitzer, Koby Crammer, Alex Kulesza, Fernando Pereira, and Jennifer Wortman Vaughan. 2018. A theory of learning from different domains. Springerlink.

Shai Ben-David and Shai Shalev-Shwartz. 2014. *Understanding Machine Learning: From Theory to Algorithms.* Cambridge University Press.

Zalán Borsos, Mojmír Mutný, and Andreas Krause. 2020. Coresets via bilevel optimization for continual learning and streaming.

Samuel R. Bowman and George E. Dahl. 2020. What will it take to fix benchmarking in natural language understanding? NAACL.

Dallas Card, Peter Henderson, Urvashi Khandelwal, Robin Jia, Kyle Mahowald, and Dan Jurafsky. 2020. With little power comes great responsibility. EMNLP.

Ciprian Corneanu, Meysam Madadi, Sergio Escalera, and Aleix Martinez. 2020. Computing the testing error without a testing set.

Weijian Deng and Liang Zheng. 2021. Are labels always necessary for classifier accuracy evaluation?

Jacob Devlin, Ming-Wei Chang, Kenton Lee, and Kristina Toutanova. 2018. Bert: Pre-training of deep bidirectional transformers for language understanding.

William B Dolan and Chris Brockett. 2004. Automatically constructing a corpus of sentential paraphrases. International Workshop on Paraphrasing.

Zeyad Ali Sami Emam, Hong-Min Chu, Ping-Yeh Chiang, Wojciech Czaja, Richard Leapman, Micah Goldblum, and Tom Goldstein. 2019. Active learning at the imagenet scale.

Kawin Ethayarajh, Yejin Choi, and Swabha Swayamdipta. 2022. Understanding dataset difficulty with v-usable information. ICML.

Sebastian Farquhar, Yarin Gal, and Tom Rainforth. 2021. On statistical bias in active learning: How and when to fix it.

Dan Feldman. 2020. Introduction to core-sets: an updated survey.

Arnav Gudibande, Eric Wallace, Charlie Snell, Xinyang Geng, Hao Liu, Pieter Abbeel, Sergey Levine, and Dawn Song. The false promise of imitating proprietary llms. *arXiv*.

Chengcheng Guo, Bo Zhao, and Yanbing Bai. 2022. Deepcore: A comprehensive library for coreset selection in deep learning.

Kelvin Guu, Albert Webson, Ellie Pavlick, Lucas Dixon, Ian Tenney, and Tolga Bolukbasi. 2023. Simfluence: Modeling the influence of individual training examples by simulating training runs. arXiv.

Pengcheng He, Xiaodong Liu, Jianfeng Gao, and Weizhu Chen. 2021. Deberta: Decoding-enhanced bert with disentangled attention.

Dan Hendrycks, Collin Burns, Steven Basart, Andy Zou, Mantas Mazeika, Dawn Song, and Jacob Steinhardt. 2021. Measuring massive multitask language understanding. *NAACL*.

Neil Houlsby, Ferenc Huszár, Zoubin Ghahramani, and Máté Lengyel. 2011. Bayesian active learning for classification and preference learning.

Jeff Bilmes Kai Wei, Rishabh Iyer. 2015. Submodularity in data subset selection and active learning.

Leonard Kaufman and Peter J Rousseeuw. 2009. *Finding groups in data: an introduction to cluster analysis*. John Wiley & Sons.

Douwe Kiela, Max Bartolo, Yixin Nie, Divyansh Kaushik, Atticus Geiger, Zhengxuan Wu, Bertie Vidgen, Grusha Prasad, Amanpreet Singh, Pratik Ringshia, Zhiyi Ma, Tristan Thrush, Sebastian Riedel, Zeerak Waseem, Pontus Stenetorp, Robin Jia, Mohit Bansal, Christopher Potts, and Adina Williams. 2021. Dynabench: Rethinking benchmarking in nlp. *NAACL*.

Krishnateja Killamsetty, Durga Sivasubramanian, Ganesh Ramakrishnan, Abir De, and Rishabh Iyer. 2021a. Grad-match: Gradient matching-based data subset selection for efficient deep model training.

Krishnateja Killamsetty, Durga Sivasubramanian, Ganesh Ramakrishnan, and Rishabh Iyer. 2021b. Glister: Generalization based data subset selection for efficient and robust learning.

Andreas Kirsch, Tom Rainforth, and Yarin Gal. 2021. Test distribution-aware active learning: A principled approach against distribution shift and outliers.

Andreas Kirsch, Joost van Amersfoort, and Yarin Gal. 2019. Batchbald: Efficient and diverse batch acquisition for deep bayesian active learning.

Jannik Kossen, Sebastian Farquhar, Yarin Gal, and Tom Rainforth. 2021a. Active surrogate estimators: An active learning approach to label-efficient model evaluation.

Jannik Kossen, Sebastian Farquhar, Yarin Gal, and Tom Rainforth. 2021b. Active testing: Sample-efficient model evaluation.

Balaji Lakshminarayanan, Alexander Pritzel, and Charles Blundell. 2017. Simple and scalable predictive uncertainty estimation using deep ensembles.

David J. C. MacKay. 1992. Information-based objective functions for active data selection. *Neural Computation*.

Leland McInnes, John Healy, and James Melville. 2018. Umap: Uniform manifold approximation and projection for dimension reduction. arXiv.

Barbara Plank Mike Zhang. 2020. Cartography active learning. *EMNLP*.

John Miller, Rohan Taori, Aditi Raghunathan, Shiori Sagawa, Pang Wei Koh, Vaishaal Shankar, Percy Liang, Yair Carmon, and Ludwig Schmidt. 2021. Accuracy on the line: On the strong correlation between out-of-distribution and in-distribution generalization.

Baharan Mirzasoleiman, Jeff Bilmes, and Jure Leskovec. 2020. Coresets for data-efficient training of machine learning models.

Ethan Perez, Douwe Kiela, and Kyunghyun Cho. 2021. True few-shot learning with language models. arXiv.

Pranav Rajpurkar, Jian Zhang, Konstantin Lopyrev, , and Percy Liang. 2016. Squad: 100,000+ questions for machine comprehension of text. Association for Computational Linguistics.

Nils Reimers and Iryna Gurevych. 2019. Sentence-bert: Sentence embeddings using siamese bert-networks. EMNLP.

Pengzhen Ren, Yun Xiao, Xiaojun Chang, Po-Yao Huang, Zhihui Li, Brij B. Gupta, Xiaojiang Chen, and Xin Wang. 2021. A survey of deep active learning.

Masoud Hekmatfar Reza Zanjirani Farahani. 2009. *Facility location: concepts, models, algorithms and case studies*. Springer-Verlag Berlin Heidelberg.

Pedro Rodriguez, Joe Barrow, Alexander Miserlis Hoyle, John P. Lalor, Robin Jia, and Jordan Boyd-Graber. 2021. Evaluation examples are not equally informative: How should that change nlp leaderboards? *ACL*.

Ozan Sener and Silvio Savarese. 2017. Active learning for convolutional neural networks: A core-set approach.

Ryan Smith, Jason Fries, Braden Hancock, and Stephen Bach. 2022. Language models in the loop: Incorporating prompting into weak supervision.

Richard Socher, Alex Perelygin, Jean Wu, Christopher D Manning Jason Chuang, Andrew Ng, , and Christopher Potts. 2013. Recursive deep models for semantic compositionality over a sentiment tree-bank. Conference on Empirical Methods in Natural Language Processing.

Aarohi Srivastava and Abhinav Rastogi. 2022. Beyond the imitation game: Quantifying and extrapolating the capabilities of language models. In *arxiv*.

Swabha Swayamdipta, Roy Schwartz, Nicholas Lourie, Yizhong Wang, Hannaneh Hajishirzi, Noah A. Smith, and Yejin Choi. 2020. Dataset cartography: Mapping and diagnosing datasets with training dynamics.

Swabha Swayamdipta, Roy Schwartz, Nicholas Lourie, Yizhong Wang, Hannaneh Hajishirzi, Noah A. Smith, and Yejin Choi. 2021. Beyond marginal uncertainty: How accurately can bayesian regression models estimate posterior predictive correlations?

Rohan Taori, Ishaan Gulrajani, Tianyi Zhang, Yann Dubois, Xuechen Li, Carlos Guestrin, Percy Liang, and Tatsunori B. Hashimoto. 2023. Stanford alpaca: An instruction-following llama model.

Eric Wallace, Mitchell Stern, and Dawn Song. 2020. Imitation attacks and defenses for black-box machine translation systems. *EMNLP*.

Alex Wang, Amanpreet Singh, Julian Michael, Felix Hill, Omer Levy, and Samuel R. Bowman. 2019. Glue: A multi-task benchmark and analysis platform for natural language understanding. ICLR.

Yizhong Wang, Yeganeh Kordi, Swaroop Mishra, Alisa Liu, Noah A. Smith, Daniel Khashabi, and Hannaneh Hajishirzi. 2023. Self-instruct: Aligning language models with self-generated instructions.

Alex Warstadt, Amanpreet Singh, and Samuel R Bowman. 2018. Neural network acceptability judgments.

Adina Williams, Nikita Nangia, and Samuel R. Bowman. 2018. A broad-coverage challenge corpus for sentence understanding through inference. Association for Computational Linguistics: Human Language Technologies.

Zhengxuan Wu, Christopher Manning, and Christopher Potts. 2023. Recogs: How incidental details of a logical form overshadow an evaluation of semantic interpretation. In *arxiv*.

Sang Michael Xie, Shibani Santurkar, Tengyu Ma, and Percy Liang. 2023. Data selection for language models via importance resampling. arXiv.

Kaichao You, Yong Liu, Jianmin Wang, and Mingsheng Long. 2021. Logme: Practical assessment of pretrained models for transfer learning.

Zhuosheng Zhang, Aston Zhang, Mu Li, and Alex Smola. 2022a. Automatic chain of thought prompting in large language models. arXiv.

Zhuosheng Zhang, Aston Zhang, Mu Li, and Alex Smola. 2022b. Automatic chain of thought prompting in large language models.

Ruiqi Zhong, Dhruba Ghosh, Dan Klein, and Jacob Steinhardt. 2021. Are larger pretrained language models uniformly better? comparing performance at the instance level.

	Random	AP Weighted	AP Predictor
SST-2	0.668	**0.744**	0.714
QQP	0.606	**0.729**	0.701
RTE	0.335	0.372	**0.453**
QNLI	0.449	**0.514**	0.312
MRPC	0.648	**0.711**	0.668
MNLI	0.302	0.366	**0.411**
Average	0.502	**0.573**	0.543

Table 4: Area Under the (Kendall's τ) Correlation Curve from 1 to 30 points for ranking the accuracy of 15 OPENAI model-prompt pairs on 6 GLUE datasets. We randomly select 10 free, open-source models to be source models for the AP methods and rank the remaining 7 models, averaging over 100 randomized runs. The best score is **bolded**. We observe that APW and APP have an average improvement over random by 0.07 and 0.04 AUCC respectively. This highlights that the anchor point methods can reduce the cost of ranking expensive target models with minimal source model costs.

A Anchor Points Generalization Analysis

We perform further investigations to assess under what conditions the predictive correlations of source models generalize well to target models. Figure 7 shows how well strong positive and strong negative trends in source model predictions generalize to target model predictions. We observe that positive trends generalize more reliably than negative trends. Negative trends suggest that models struggle to correctly label both of two examples correctly: greater confidence in the correct class in one example correlates with lesser confidence in the correct class of the other example. We hypothesize that this characteristic is a weakness of some models that does not generalize to stronger models, leading to poor generalization. Note that Equation 1 selects points with strong positive trends, avoiding this issue.

Figure 8 shows the correlation matrix of 50 randomly selected SST-2 points, computed across the predictions of all 87 models. We observe that nearly all correlations are positive, with a notable exception. This exception is a highly contentious example: "we root for (clara and paul) , even like them , though perhaps it 's an emotion closer to pity, " labeled as positive sentiment. We observe in Figure 8(b) that prompted language models tend to follow a negative trend between this example and others, while fine-tuned BERT models do not. This suggests a distinction in how fine-tuned and prompted models fit the task distribution. Notably, it highlights that different model families may have predictive correlations that do not generalize to other families. Further analysis of these properties could lead to the design of intelligent source selection schemes for evaluating a given set of target models.

Figures 15 and 16 show the Kendall tau correlation curves for the various model ranking methods. For many settings, APW correlation begins to plateau as the evaluation set size grows to 100 points. For 19 of the 30 settings, the random selection curve eventually reaches the APW curve at some evaluation set size smaller than 100 points. This is natural: a randomly-selected evaluation set is sufficiently representative when sufficiently large. These diminishing returns occur more quickly for simpler datasets (e.g. SST-2) and less so for more complex datasets (e.g. MNLI), reflecting that more complex distributions require larger evaluation sets to be well-represented. However, it is surprising that random selection eventually *surpasses* the APW curve in 5 of these 19 settings. This is a result of the APW curve having a tighter upper bound than random selection: in the limit where $|\mathcal{X}_{acq}| = |\mathcal{X}_{eval}|$, instance-level confidence in the correct class averaged over the entire dataset does not perfectly correlate with accuracy over the entire dataset. This upper bound does not exist for APP.

B Anchor Points for Ranking Massive Multitask Language Understanding

Model
1. huggyllama/llama-7b
2. huggyllama/llama-13b
3. mosaicml/mpt-7b
4. tiiuae/falcon-7b
5. facebook/opt-350m
6. facebook/opt-125m
7. facebook/opt-6.7B
8. mistralai/Mistral-7B-Instruct-v0.1
9. Eleuther/pythia-12b
10. openlm-research/open_llama_7b
11. meta-llama/Llama-2-7b
12. openlm-research/open_llama_3b
13. openlm-research/open_llama_7b
14. openlm-research/open_llama_13b

Table 8: LLMs used for MMLU experiments. Models can be accessed at https://huggingface.co/models.

We perform a small scale experiment to evaluate anchor points at ranking models on 6 Massive Multitask Language Understanding (Hendrycks et al., 2021) datasets: clinical knowledge, college chemistry, college physics, global facts, high school European history, and high school physics. Each dataset contains multiple choice questions requiring extensive real-world knowledge. Table 6 shows results of the Anchor Point Predictor, Anchor Point Weighted, and baselines at ranking 7 target models using 7 source models with 1-30 anchor points. Due to the complexity of these tasks, we substitute the fine-tuned BERT embedding baselines with BAAI/bge-large-en-v1.5, a state-of-the-art embedding model.

We find that Anchor Points Weighted is the strongest performer overall, outperforming random selection on 5 of the 6 datasets with an average improvement of 0.07 AUCC. However, the Anchor Points Predictor outperforms random on only 3 of 6 datasets. Notably, both methods are far below random on the Global Facts dataset. This is perhaps due to the randomness and specificity of the Global Facts questions: many have answers that are likely to be rare in pre-training data, such as 'What is the percentage of children aged 13-15 in the United States who reported being bullied at least once in the past couple of months as of 2015?" The correlations learned between these questions (using only 7 source models) are likely to be weak or spurious. Increasing the source model set size would improve the probability of learning generalizable predictive correlations.

Interestingly, the improved performance of Pretrained Weighted in MMLU relative to GLUE suggests that semantic similarity in questions can be an effective proxy of model performance similarity when questions emphasize intensive knowledge rather than simple language understanding. However, the inconsistency of these approaches still warrants a more reliable technique such as Anchor Points Weighted.

C Hyperparameters, Compute, and Packages

For each GLUE task, we finetune all BERT-family with a batch size of 32, learning rate of 2e-5, and weight decay of 0.01 for 3 epochs. We did not perform extensive hyperparameter tuning; thus, model performances do not necessarily represent their ideal performance. We chose to not perform hyperparameter tuning in order to assess whether anchor points could reliably evaluate models with a wide range of performances. This training process, as well as the process of training code development and model inference, took approximately 120 GPU

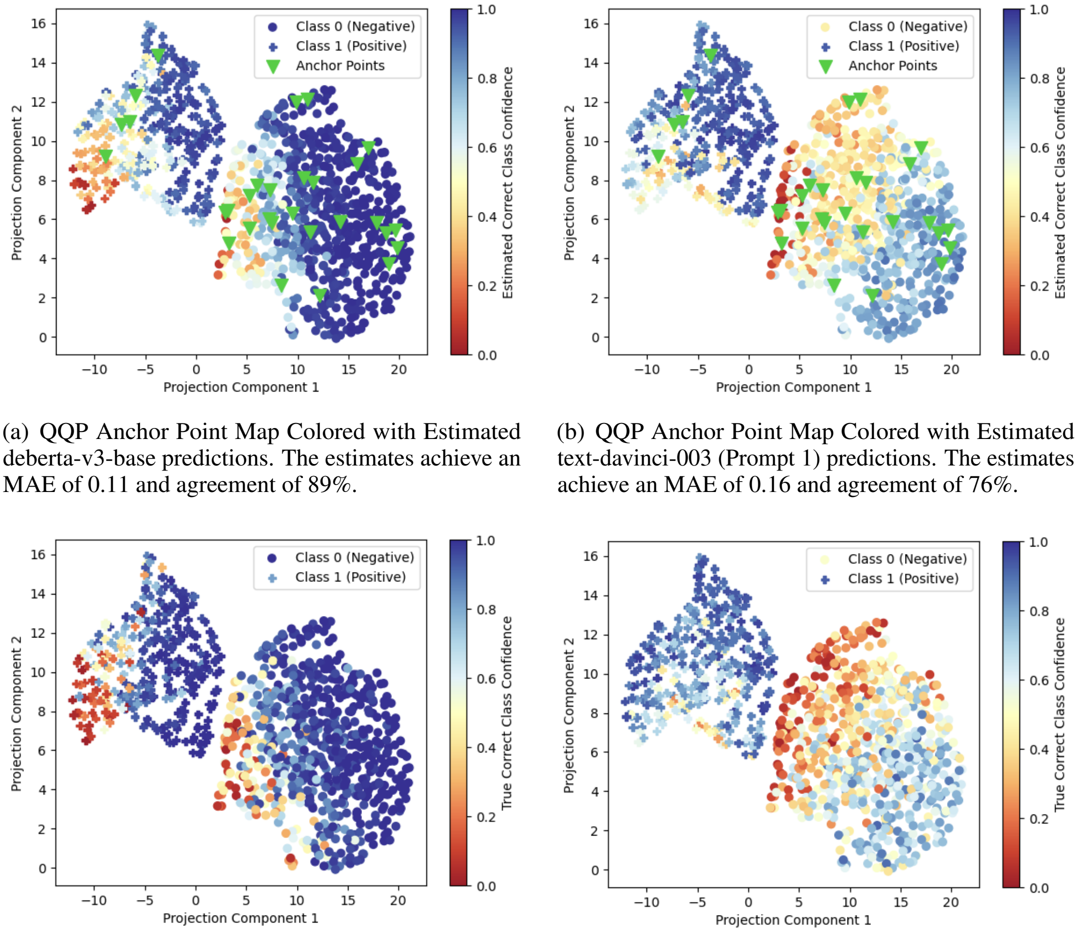

(a) QQP Anchor Point Map Colored with Estimated deberta-v3-base predictions. The estimates achieve an MAE of 0.11 and agreement of 89%.

(b) QQP Anchor Point Map Colored with Estimated text-davinci-003 (Prompt 1) predictions. The estimates achieve an MAE of 0.16 and agreement of 76%.

(c) QQP Anchor Point Map Colored with True deberta-v3-base predictions.

(d) QQP Anchor Point Map Colored with True text-davinci-003 (Prompt 1) predictions.

Figure 5: Anchor Point Map for 1000 QQP examples. The map is computed using the predictions of 60 randomly-selected source models. We then estimate the predictions of the two held-out target models, deberta-v3-base and text-davinci-003, by evaluating each on 30 anchor points. We color the remaining 970 test points in 5(a) and 5(b) with these estimates. Finally, we color maps 5(c) and 5(d) with the true target model predictions. We observe that the estimated predictions achieve low MAE and high agreement with the true predictions.

	Nearest Source Neighbor				Anchor Points			
Dataset	$N = 5$	$N = 10$	$N = 30$	$N = 50$	$N = 5$	$N = 10$	$N = 30$	$N = 50$
SST-2	$0.78_{0.19}$	$0.83_{0.16}$	$0.86_{0.12}$	$0.87_{0.12}$	$0.78_{0.15}$	$0.83_{0.12}$	$0.85_{0.11}$	$0.85_{0.12}$
QQP	$0.77_{0.21}$	$0.84_{0.15}$	$0.87_{0.13}$	$0.88_{0.13}$	$0.79_{0.15}$	$0.81_{0.13}$	$0.84_{0.11}$	$0.85_{0.12}$
RTE	$0.74_{0.24}$	$0.80_{0.21}$	$0.84_{0.18}$	$0.86_{0.16}$	$0.78_{0.19}$	$0.83_{0.17}$	$0.80_{0.18}$	$0.87_{0.16}$
QNLI	$0.73_{0.22}$	$0.78_{0.19}$	$0.83_{0.17}$	$0.83_{0.16}$	$0.69_{0.17}$	$0.76_{0.17}$	$0.77_{0.17}$	$0.77_{0.16}$
MRPC	$0.77_{0.16}$	$0.80_{0.15}$	$0.82_{0.15}$	$0.83_{0.15}$	$0.75_{0.15}$	$0.79_{0.14}$	$0.85_{0.10}$	$0.81_{0.15}$
MNLI	$0.65_{0.27}$	$0.71_{0.26}$	$0.76_{0.24}$	$0.78_{.24}$	$0.76_{0.20}$	$0.79_{0.20}$	$0.80_{0.20}$	$0.79_{0.20}$
Average	0.74	0.79	0.83	0.84	0.76	0.80	0.82	0.82

Table 5: Anchor Point Agreement for Various Source Model Set Sizes on GLUE. We assess Nearest Source Neighbor and Anchor Points using $B = 10$ points in all settings. We observe that Anchor Points are the stronger performer for smaller source model sets, but are surpassed by Nearest Source Neighbor for larger sets. Note that anchor points are stronger across the board for MNLI and weaker across the board for QNLI, indicating that the nature of the dataset plays a large role.

	Random	Random Mean	Pretrained	Pretrained Weighted	BGE	BGE Weighted Weighted	AP Weighted	AP Predictor
Datasets	Exact	Corr	Exact	Corr	Exact	Corr	Corr	Exact
Clinical Knowledge	0.532	0.638	0.593	0.705	0.542	0.491	**0.711**	0.640
College Chemistry	0.390	0.445	0.148	0.332	0.384	0.472	**0.477**	0.267
College Physics	0.251	0.280	0.310	0.206	0.077	0.30	**0.343**	0.130
Global Facts	0.251	0.116	0.117	0.118	**0.384**	0.109	0.151	0.052
HS Euro. History	0.596	0.656	0.612	0.678	0.677	**0.741**	0.667	0.620
HS Physics	0.245	0.215	0.307	**0.339**	-0.014	-0.27	0.324	0.307
Average	0.378	0.392	0.350	0.406	0.341	0.262	**0.445**	0.336

Table 6: Area Under the (Kendall's τ) Correlation Curve from 1 to 30 points for ranking the accuracy of 7 language models on 6 MMLU datasets. We randomly select 7 models (see Table 8) to be source models for the AP methods and rank the remaining 7 models, averaging over 100 randomized runs. "Exact" indicates the method generates a score that is intended to approximate the true aggregate performance directly, while "Corr" indicates the method generates a score intended only to rank correlate with true performance. The best score is **bolded** and second best score is underlined.

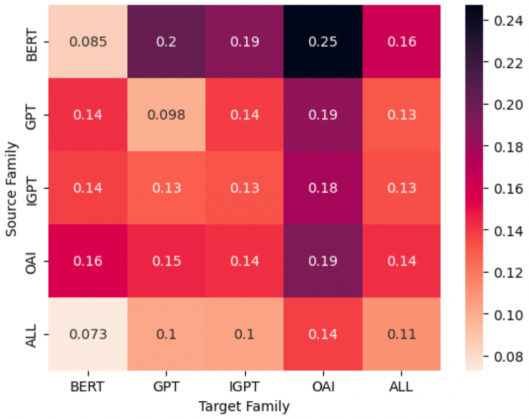

Figure 6: Transfer table showing the mean absolute error of trend lines fit to the instance-level predictions of one model family and used to estimate the instance-level predictions of another family. Along the diagonal, we partition the family into source and target halves randomly. Results are averaged over 1000 points pairs from each of the 6 GLUE tasks. Point pairs are randomly selected from all pairs having a Pearson correlation greater than +0.8 within the source model predictions.

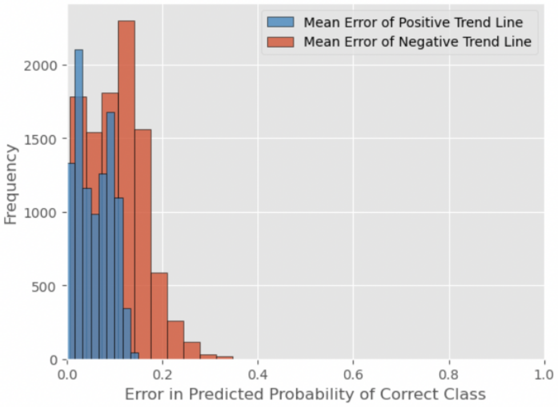

Figure 7: Mean Absolute Error Distribution for regression lines fit to source model predictions with moderate-to-strong fit ($R^2 > 0.64$) and used to predict target model predictions. Generalization is worse for trends with negative slopes.

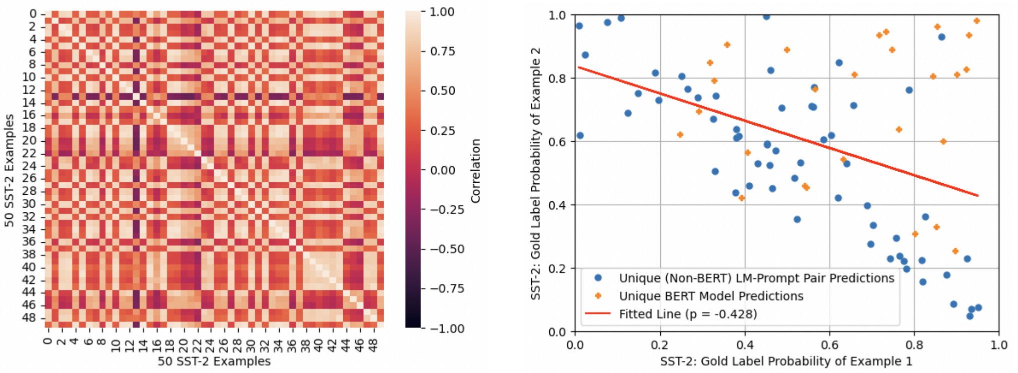

(a) Pairwise Correlation Matrix of 87 Model-Prompt Pairs Correct Class Confidences on 50 SST-2 Examples. Rich structure indicates the relatedness of various examples. Notably, a dark bar at index 13 indicates an example that tends to negatively correlate with all other examples.

(b) Correct Class Confidences of 87 Models on Two Selected SST-2 sentence pair examples. Example 1 (x-axis) corresponds to the dark bar in 8(a), a highly contentious example. Prompted models follow a negative trend while BERT models follow no trend, highlighting the distinct behavior of fine-tuned vs. prompted models.

Figure 8: Predictive Correlations at the Instance-Level Across Language Models: SST-2 Case Study

hours with a single A100.

We used Sentence Transformers 2.2.2, Scipy 1.10.1, transformers 4.25.1, tokenizers 0.11.4, numpy 1.23.5, scikit-learn 1.2.2, kmedoids 0.4.3, and the Eleuther Evaluation Harness (https://github.com/EleutherAI/lm-evaluation-harness).

D Prompts

We enumerate the zero-shot prompts used for each dataset below. All prompts are randomly selected from Prompt Source (Bach et al., 2022)

QQP

1. Can an answer to "{{question1}}" also be used to answer "{{question2}}"?

2. I received the questions "{{question1}}" and "{{question2}}". Are they duplicates?

3. Are the questions "{{question1}}" and "{{question2}}" asking the same thing?

SST-2

1. Does the following sentence have a {{"positive"}} or {{"negative"}} sentiment? {{sentence}}

2. Someone just said to me "{{sentence}}". Do you think they are {{"sad"}} or {{"happy"}}?’

3. I'm reading a review that says "{{sentence}}". Do you think the review is {{"positive"}} or {{"negative"}}?

RTE

1. Does the claim "{{sentence2}}" follow from the fact that "{{sentence1}}"? Please answer either {{"yes"}} or {{"no"}}

2. Is the relationship from the first to the second sentence "{{"entailment"}}" or "{{"not entailment"}}"?

3. Does "{{sentence1}}" imply that "{{sentence2}}"? Please answer either {{"yes"}} or {{"no"}}

QNLI

1. Can you answer the question "{{question}}" based only on the following: {{sentence}}

2. {{sentence}} Does that sentence have all you need to answer the question "{{question}}"?

3. Does knowing that "{{sentence}}" imply that I know the answer to "{{question}}

MNLI

1. Suppose it's true that {{premise}} Then, is "{{hypothesis}}" {{"always"}}, {{"sometimes"}}, or {{"never"}} true?

2. Question: {{hypothesis}} True, False, or Neither?

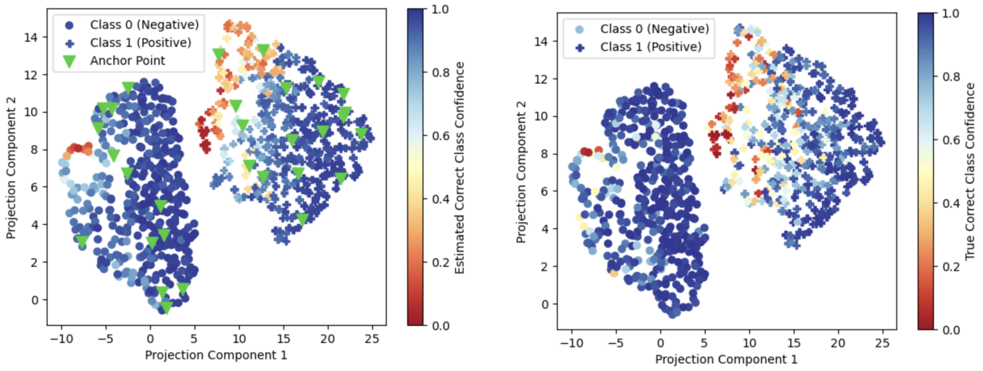

(a) SST-2 Anchor Point Map Colored with Estimated Falcon-7b (Prompt 3) Predictions. The estimates achieve an MAE of 0.09 and agreement of 92%.

(b) SST-2 Anchor Point Map Colored with True Falcon-7b (Prompt 3) Predictions.

Figure 9: SST-2 Validation Set Anchor Point Map. The locations of all 872 points are learned using the predictions of 60 randomly-selected source models on SST-2. We then evaluate Falcon-7b (held-out) on 30 anchor points, shown by green triangles in 9(a). Next, the model's predictions on only these anchor points is used to estimate the models' predictions on the remaining 842 points, with a mean absolute error of 0.09 and 92% agreement with the true predictions. The estimates are also shown in 9(a). achieving 0.09 MAE and 92% agreement with the models' true predictions. Finally, we color the Anchor Point Map with Falcon-7B's true predictions in 9(b). The estimated predictions successfully identify regions where the model is weak (red regions).

3. {{premise}} Using only the above description and what you know about the world, "{{hypothesis}}" is definitely correct, incorrect, or inconclusive?

MRPC

1. {{sentence1}} paraphrase (that is, mean the same thing as) this sentence? {{sentence2}}
2. Can I replace the sentence {{sentence1}} with the sentence {{sentence2}} and have it mean the same thing?
3. Are the following two sentences "{{"equivalent"}}" or "{{"not equivalent"}}"? {{sentence1}} {{sentence2}}

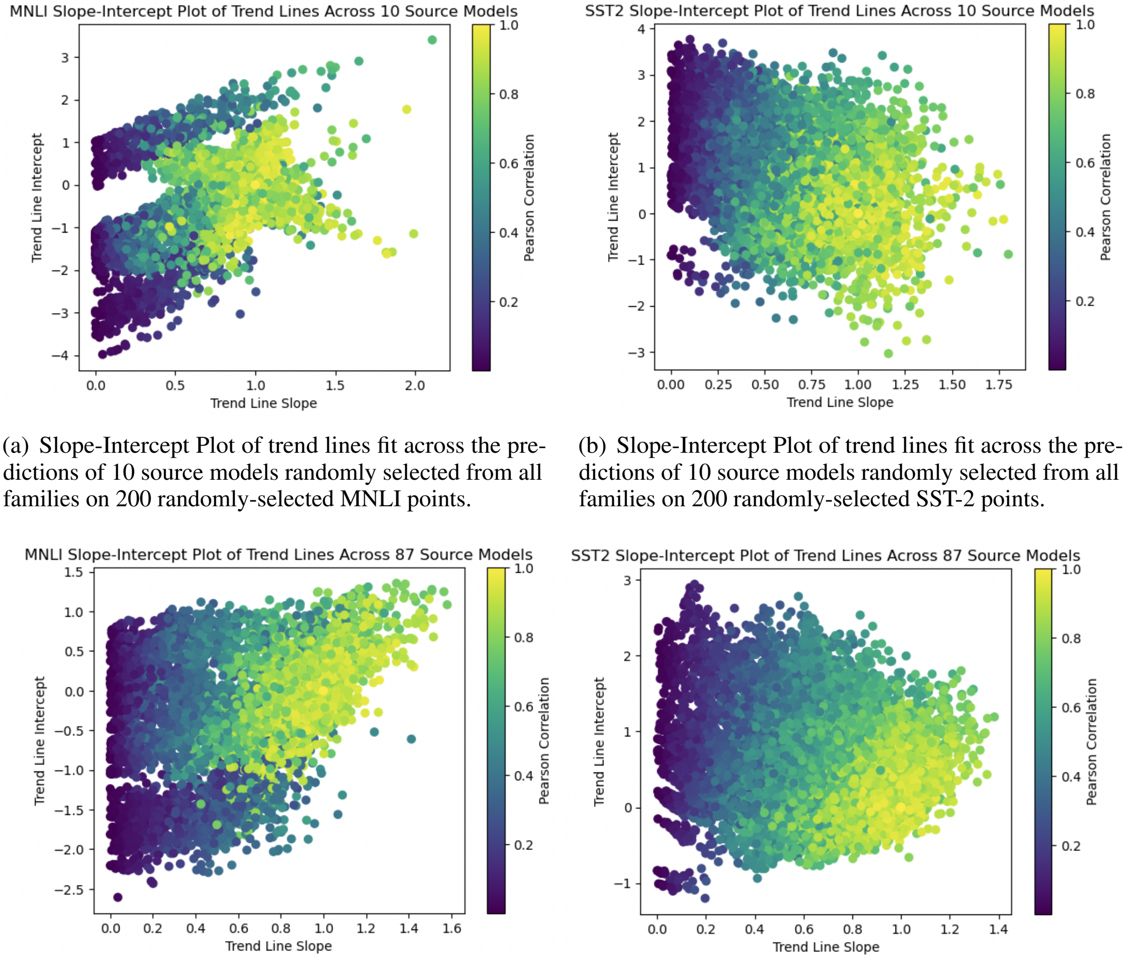

(a) Slope-Intercept Plot of trend lines fit across the predictions of 10 source models randomly selected from all families on 200 randomly-selected MNLI points.

(b) Slope-Intercept Plot of trend lines fit across the predictions of 10 source models randomly selected from all families on 200 randomly-selected SST-2 points.

(c) Slope-Intercept Plot of trend lines fit across the predictions of 87 source models from all families on 200 randomly-selected MNLI points.

(d) Slope-Intercept Plot of trend lines fit across the predictions of 87 source models from all families on 200 randomly-selected SST-2 points.

Figure 10: Slope-Intercept Plots of Trend Lines Fit Across the Predictions of Source Models on all pairs of 200 points randomly selected from MNLI and SST-2. Note that high Pearson correlations naturally emerge when trend lines have a slope near one and intercept near zero. This holds even when the number of source models is small (e.g. 10), suggesting that spuriously high correlations are not common.

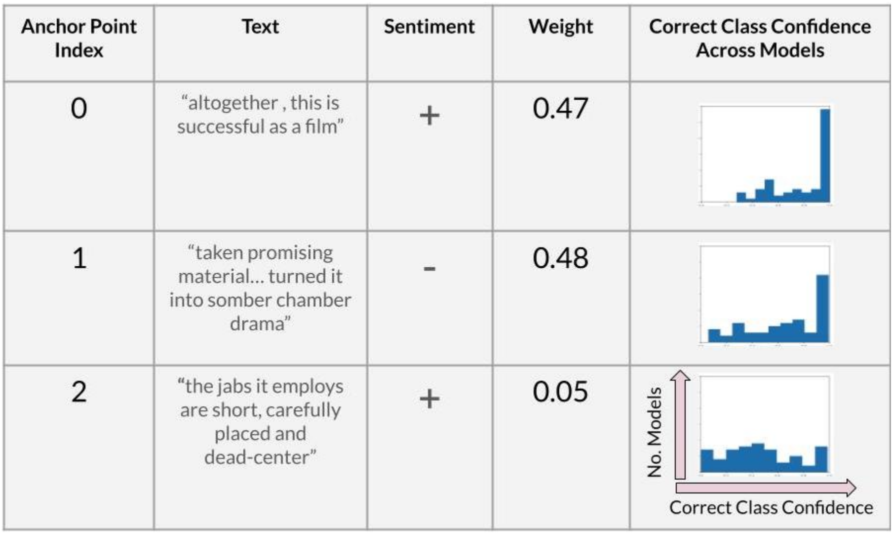

Anchor Point Index	Text	Sentiment	Weight	Correct Class Confidence Across Models
0	"altogether , this is successful as a film"	+	0.47	
1	"taken promising material... turned it into somber chamber drama"	-	0.48	
2	"the jabs it employs are short, carefully placed and dead-center"	+	0.05	

No. Models
Correct Class Confidence

Figure 11: Anchor point sets can be highly representative despite being small. This figure shows three SST-2 Anchor Points. The Anchor Point Weighted Score computed using these three points achieves a Kendall Tau correlation of 0.68 with true model performance on the SST-2 validation set (872 points), sufficient to identify the stronger performer of a randomly selected pair of models with 84% probability. (Evaluating the pair on three randomly selected points would identify the stronger performer with 67% probability). By observing the distribution of the correct class confidence of many models on these three points, we see that these points correspond to easy (0), moderate (1), and difficult (2) examples.

Algorithm 1 Anchor Points Predictor Fit

```
$K \leftarrow$ number of anchor points
$P \leftarrow NxDxQ$ tensor of $N$ source models' output probabilities on $D$ points over $Q$ classes
$P \leftarrow logit(P)$                                   ▷ take logit transform of predictions
$M \leftarrow$ empty $(D-K) \times K \times Q$ array        ▷ To store slopes
$B \leftarrow$ empty $(D-K) \times K \times Q$ array        ▷ To store biases
$R \leftarrow$ empty $(D-K) \times K \times Q$ array        ▷ To store residuals
$N \leftarrow$ empty $(D-K) \times K \times Q$ array        ▷ Zero-initialized tensor to indicate nearest anchors
$C \leftarrow$ sum([corrcoef($P[:,:,i]$ for $i$ in range($Q$)]) / $Q$   ▷ $D \times D$ averaged correlation matrix
$AP \leftarrow$ K-MEDOIDS(1 - C, K)                       ▷ length K array of anchor point indices
$T \leftarrow \{0...D-1\} \setminus AP$                   ▷ length D - K array of test point indices
for q in range(Q) do
    for i, test $\in$ enumerated $T$ do
        for j,anchor $\in$ enumerated $AP$ do
            $x \leftarrow$ P[:,j,q]
            $y \leftarrow$ P[:,i,q]
            m, b, r $\leftarrow$ LinearRegression(x, y)   ▷ Slope, bias, and residual of trend line
            M[i,j,q] $\leftarrow$ m
            B[i,j,q] $\leftarrow$ b
            R[i,j,q] $\leftarrow$ r
        end for
    end for
    nearest $\leftarrow$ argmin(R[:,:,q], axis = 1)       ▷ nearest anchor indices to each point
    N[arange(D-K),nearest,q] $\leftarrow$ 1               ▷ populate indicator array
end for
     return AP, N, T, M, B
```

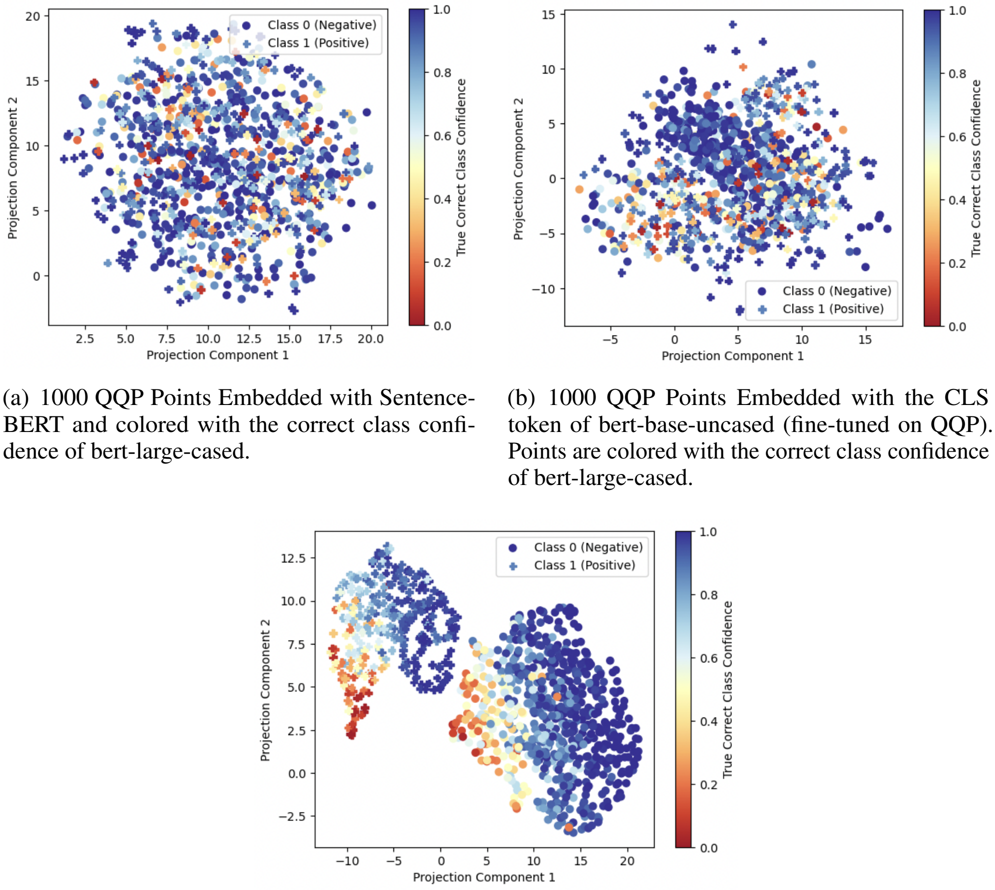

(a) 1000 QQP Points Embedded with Sentence-BERT and colored with the correct class confidence of bert-large-cased.

(b) 1000 QQP Points Embedded with the CLS token of bert-base-uncased (fine-tuned on QQP). Points are colored with the correct class confidence of bert-large-cased.

(c) 1000 QQP Points Visualized with the Anchor Point Map using 60 source models and colored with the correct class confidence of bert-large-cased.

Figure 12: Comparison of model performance trends within various embedding spaces. Only the Anchor Points Map results in clean localization of model performance where a held-out model's performance on each point correlates with its performance on neighboring points. This allows fine-grained comparison of how different models perform on the same dataset distribution.

Algorithm 2 Anchor Points Predictor Predict

```
Require: AP, N, T, M, B                                        ▷ Returned by Anchor Points Fit
  P ← length K array of a target model's gold label predictions on the K anchor points
  $P$ ← logit(P)     ▷ take logit transform of predictions    ▷ To store estimated target model predictions
  preds ← (M * P[newaxis,:,:] + B)                                              ▷ Prediction step
  preds ← sum(preds * N, axis = 1)                        ▷ Prune predictions from non-nearest anchors
  Y ← expit(preds)                                                  ▷ Inverse of the logit transform
      return Y
```

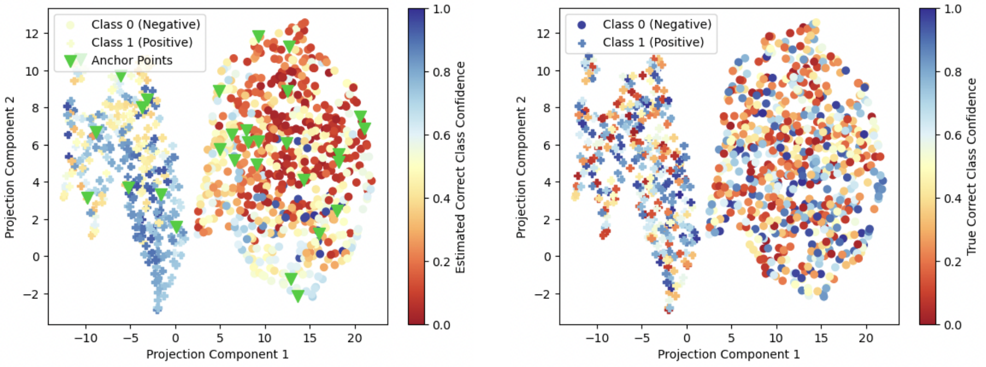

(a) QQP Anchor Point Map Colored with Estimated text-curie-001 (Prompt 1) predictions. The estimates achieve a large MAE of 0.30 and poor agreement of 54%.

(b) QQP Anchor Point Map Colored with True text-curie-001 (Prompt 1) predictions.

Figure 13: Anchor Point Failure Case: The map is computed using the predictions of 60 randomly-selected source models on QQP and used to estimate the predictions of text-curie-001 with Prompt 1 (13(a)). The estimates achieve a large MAE and near random agreement. Upon inspecting the true predictions (13(b)), we observe that the behavior of text-curie-001 is not localized in the Anchor Point Map. Model performance appears sporadic. This suggests that text-curie-001 does not follow the same predictive correlations as the source models, preventing effective estimation of the model's predictions.

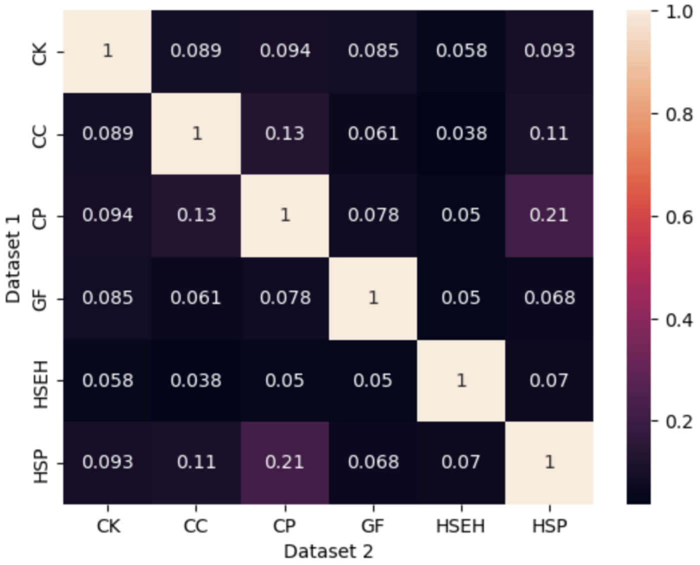

Figure 14: Vocabulary overlap of our MMLU datasets. Each cell indicates the portion of words in dataset 1 that are also in dataset 2. Labels: CK = clinical knowledge, CC = college chemistry, CP = college physics, GF = global facts, HSEH = high school European history, HSP = high school physics.

	Mean	Random	Random Weighted	Pretrained	Pretrained Weighted	Fine-Tuned	Fine-Tuned Weighted	AP Weighted	AP Predictor
Datasets	Family	Exact	Corr	Exact	Corr	Exact	Corr	Corr	Exact
SST-2	BERT	0.485	0.607	0.512	0.637	0.594	**0.738**	0.696	0.593
QQP	BERT	0.459	0.631	0.670	0.613	0.572	**0.756**	0.691	0.555
RTE	BERT	0.478	0.406	0.316	-0.001	0.486	0.335	0.591	**0.597**
QNLI	BERT	0.346	0.523	-0.252	0.613	-0.430	0.510	**0.665**	0.571
MRPC	BERT	0.730	0.741	0.737	0.749	0.692	**0.786**	0.778	0.721
MNLI	BERT	0.684	0.748	0.646	0.653	0.676	**0.735**	0.733	0.720
BERT Avg.		0.530	0.609	0.438	0.543	0.432	0.643	**0.699**	0.626
SST-2	GPT	0.440	0.278	0.548	0.215	**0.651**	0.531	0.441	0.632
QQP	GPT	0.561	0.591	-0.557	-0.537	0.720	0.752	0.777	**0.825**
RTE	GPT	0.188	0.138	-0.119	-0.251	0.133	0.082	0.378	**0.452**
QNLI	GPT	0.101	0.076	0.209	0.197	0.185	0.130	**0.158**	0.126
MRPC	GPT	0.475	0.460	0.155	0.321	0.360	0.360	0.516	**0.681**
MNLI	GPT	0.033	0.059	-0.517	-0.382	0.181	0.099	0.201	**0.494**
GPT Avg.	GPT	0.300	0.267	-0.470	-0.730	0.371	0.325	0.410	**0.535**
SST-2	IGPT	0.655	0.722	0.726	0.728	0.606	0.760	**0.814**	0.719
QQP	IGPT	0.734	0.801	0.264	0.276	0.824	**0.893**	0.884	0.845
RTE	IGPT	0.389	0.322	0.220	0.03	0.391	0.323	**0.671**	0.629
QNLI	IGPT	0.404	0.400	0.512	0.469	0.449	0.296	0.597	**0.690**
MRPC	IGPT	0.727	0.680	0.520	0.651	0.651	0.712	**0.776**	0.738
MNLI	IGPT	0.265	0.305	-0.074	-0.088	**0.460**	0.420	0.434	0.317
IGPT Avg.		0.529	0.538	0.361	0.344	0.563	0.566	**0.696**	0.656
SST-2	OAI	0.666	0.697	0.774	**0.871**	0.761	0.833	0.734	0.661
QQP	OAI	0.610	0.651	-0.090	-0.080	0.676	0.722	**0.747**	0.637
RTE	OAI	0.362	0.303	0.206	0.066	0.381	0.294	-0.378	**0.411**
QNLI	OAI	0.451	0.453	0.381	0.378	0.286	-0.03	**0.497**	0.309
MRPC	OAI	0.633	0.661	0.533	0.563	0.550	0.673	**0.714**	0.705
MNLI	OAI	0.300	0.278	-0.015	-0.181	0.559	**0.490**	0.350	0.486
OAI Avg.	OAI	0.503	0.507	0.298	0.270	0.536	0.497	**0.570**	0.535
SST-2	ALL	0.685	0.705	0.734	0.725	0.730	**0.787**	0.757	0.727
QQP	ALL	0.669	0.678	0.189	0.233	0.766	**0.770**	0.756	0.701
RTE	ALL	0.366	0.308	0.143	-0.052	0.354	0.275	**0.483**	0.462
QNLI	ALL	0.321	0.331	0.192	0.294	0.127	0.144	**0.439**	0.303
MRPC	ALL	0.687	0.679	0.528	0.604	0.641	0.681	**0.726**	0.716
MNLI	ALL	0.438	0.433	0.177	0.166	0.523	0.453	**0.544**	0.517
Avg.	ALL	0.528	0.522	0.327	0.328	0.523	0.518	**0.612**	0.571

Table 7: Area Under the (Kendall's τ) Correlation Curve from 1 to 30 points for ranking language models at 6 GLUE tasks from each model family. We randomly select 5 source models each for the InstructGPT and OpenAI Families and 10 each for the BERT, GPT, and ALL families. We then rank the remaining models within each family and average over 100 randomized runs. AP Weighted and AP Predictor prove to be the most effective at accurately ranking models in this small-data regime. In each row, the best score is **bolded** and second best score is underlined.

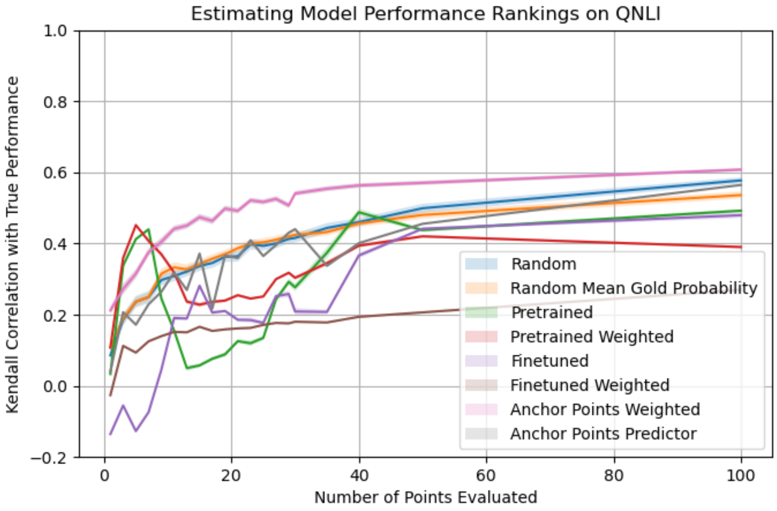

(a) QNLI

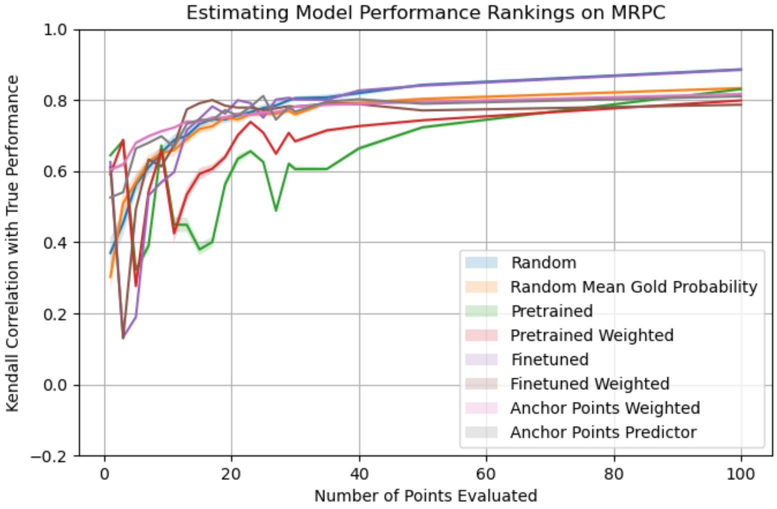

(b) MRPC

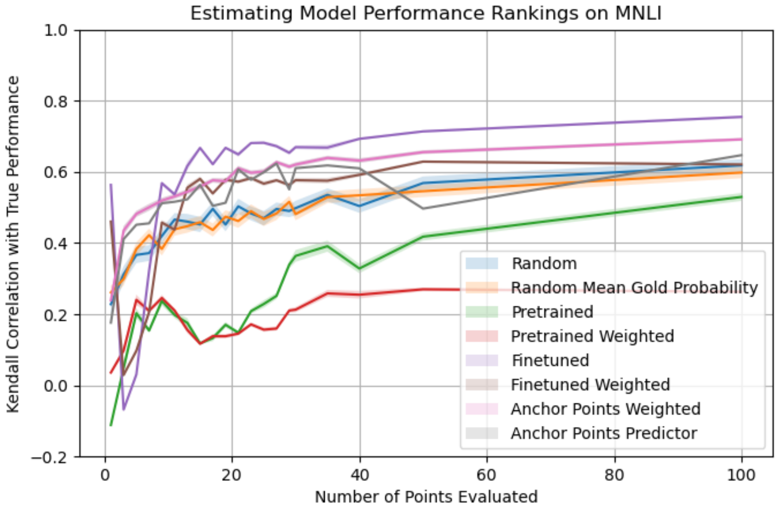

(c) MNLI

Figure 15: Kendall Tau Rank Correlation between Model Rankings on Small Evaluation Sets and Full Validation Sets for QNLI, MRPC, and MNLI. We rank 77 language models belonging to all model families using various evaluation selection techniques. Anchor Points are fit to 10 source model predictions. Each point is the mean of 100 runs with randomized source and target models. Shading indicated standard error. Anchor Points Weighted achieves the most reliable performance overall at low evaluation set sizes.

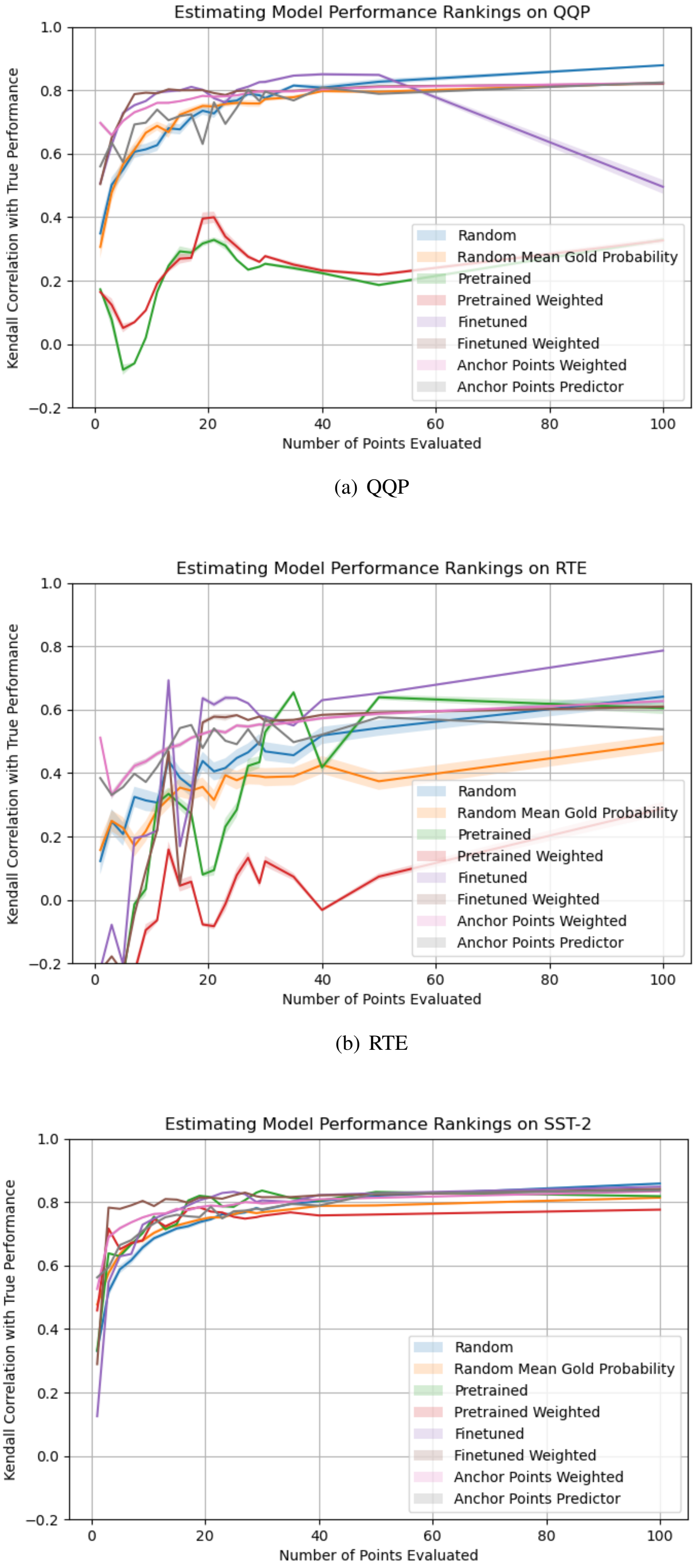

(a) QQP

(b) RTE

(c) SST-2

Figure 16: Kendall Tau Rank Correlation between Model Rankings on Small Evaluation Sets and Full Validation Sets for QQP, RTE, and SST-2. We rank 77 language models belonging to all model families using various evaluation selection techniques. Anchor Points are fit to 10 source model predictions. Each point is the mean of 100 runs with randomized source and target models. Shading indicated standard error. Anchor Points Weighted achieves the most reliable performance overall at low evaluation set sizes.

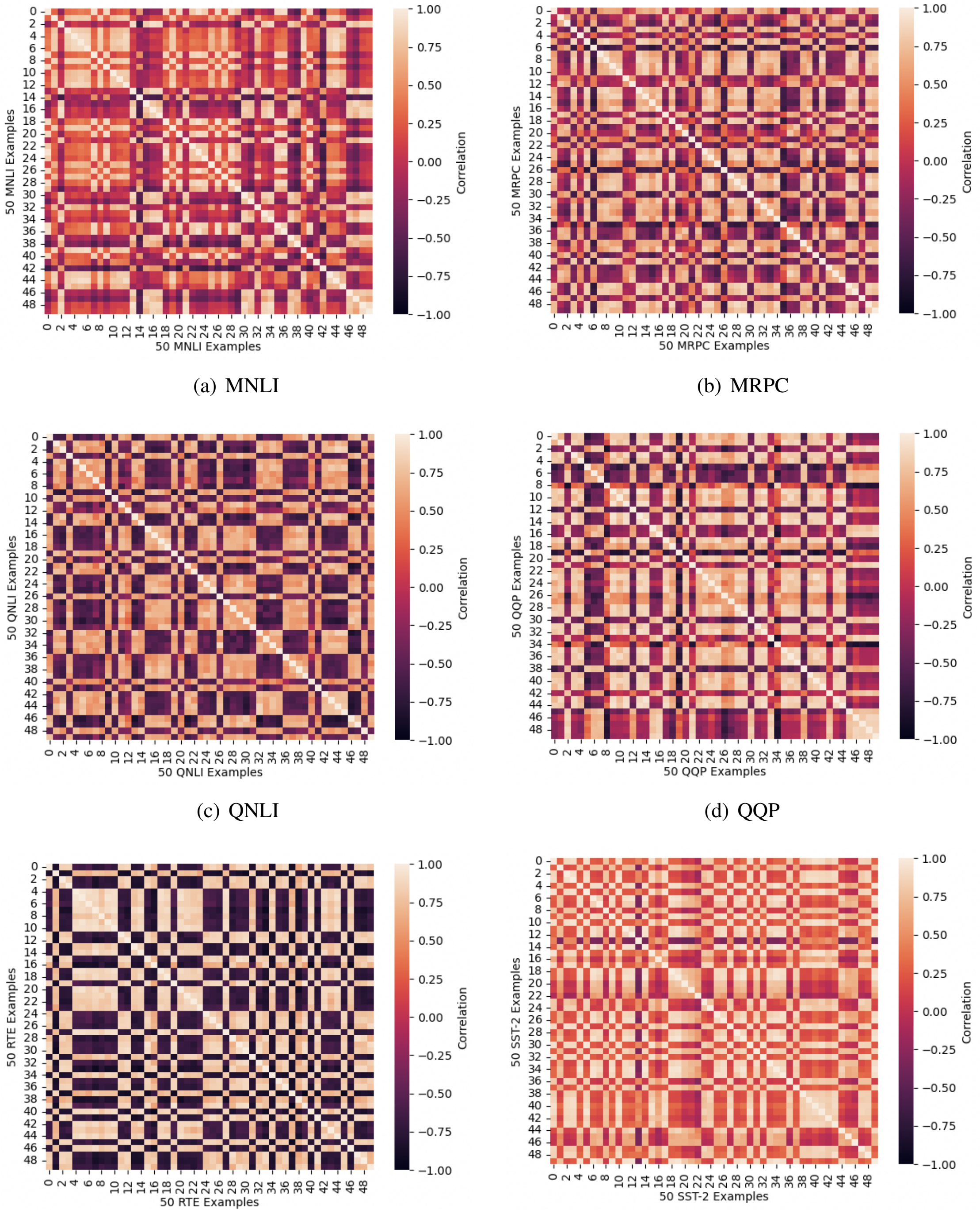

(a) MNLI

(b) MRPC

(c) QNLI

(d) QQP

(e) RTE

(f) SST-2

Figure 17: Correlation Matrices of Correct Class Confidence Predictions from 87 models across all model families. Each plot shows the correlations between 50 examples sampled from the validation Sets of GLUE Tasks.

Model	Parameter Count	MNLI	SST-2	QQP	RTE	MRPC	QNLI
1. Bio-ClinicalBERT	110M	0.502	0.875	0.815	0.472	0.384	0.595
2. albert-base-v2	11M	0.325	0.927	0.797	0.472	0.522	0.505
3. bart-base	139M	0.834	0.954	0.841	0.747	0.855	0.626
4. bart-large	400M	0.891	0.915	0.639	0.527	0.892	0.505
5. bert-base-cased	110M	0.444	0.917	0.639	0.519	0.504	0.505
6. bert-base-multilingual-cased	110M	0.478	0.890	0.828	0.472	0.392	0.505
7. bert-base-uncased	110M	0.468	0.917	0.639	0.476	0.318	0.630
8. bert-large-cased	336M	0.319	0.509	0.639	0.487	0.627	0.505
9. bert-large-uncased	336M	0.611	0.916	0.639	0.472	0.387	0.505
10. bert-mini	11M	0.479	0.845	0.819	0.476	0.664	620
11. bert-tiny	3M	0.428	0.803	0.784	0.530	0.479	0.639
12. biobert-v1.1	110M	0.539	0.894	0.825	0.50	0.540	0.617
13. deberta-base	100M	0.876	0.940	0.639	0.631	0.884	0.505
14. deberta-large	350M	0.344	0.950	0.639	0.527	0.904	0.505
15. deberta-v3-base	304M	0.320	0.950	0.850	0.837	0.880	0.663
16. deberta-v3-xsmall	22M	0.352	0.924	0.850	0.678	0.865	0.660
17. distilbert-base-cased	67M	0.820	0.90	0.831	0.570	0.818	0.618
18. distilbert-base-uncased	66M	0.820	0.896	0.840	0.570	0.830	0.613
19. electra-base-discriminator	102M	0.863	0.943	0.830	0.761	0.892	0.645
20. legal-bert-small-uncased	24M	0.415	0857	0.831	0.472	0.450	0.597
21. roberta-base	125M	0.873	0.938	0.834	0.736	0.870	0.505
22. scibert-scivocab-uncased	110M	0.528	0.891	0.830	0.550	0.436	0.599
23. sentence-bert	110M	0.413	0.919	0.8225	0.545	0.321	0.505
24. sentiment-roberta-large-english	335M	0.890	0.951	0.693	0.580	0.840	0.505
25. twitter-roberta-base	125M	0.835	0.930	0.833	0.588	0.855	0.590
26. xlm-roberta-base	279M	0.835	0.916	0.633	0.527	0.860	0.505
27. xlm-roberta-large	355M	0.353	0.509	0.639	0.602	0.884	0.505

Table 9: BERT-Family Model Accuracies on Six GLUE Tasks. Hyperparameters are in Appendix C. Models can be accessed at https://huggingface.co/models.

Model	Parameter Count
1. Cerebras-GPT-1.3B	1.3B
2. Cerebras-GPT-111M	111M
3. Cerebras-GPT-256M	256M
4. bloom-1b7	1.72B
5. gpt-neo-1.3B	1.3B
6. gpt-neo-125m	125M
7. gpt2-large	774M
8. gpt2-medium	355M
9. gpt2	137M
10. openai-gpt	120M
11. RedPajama-INCITE-Instruct-7B-v0.1	7B
12. falcon-7b-instruct	7B
13. mpt-7b-instruct	7B
14. mt0-xl	3.7B
15. bloomz-3b	3B
16. text-ada-001	Not publicly known
17. text-babbage-001	Not publicly known
18. text-curie-001	Not publicly known
19. text-davinci-002	Not publicly known
20. text-davinci-003	Not publicly known

Table 10: GPT, InstructGPT, and OpenAI Family Model Zero-Shot Models and Parameter Counts (Used for GLUE experiments). OpenAI Model parameter counts are unknown. Models can be accessed at https://huggingface.co/models and https://platform.openai.com/docs/models.